Review article

Yiwei Xie, Zihan Geng, Leimeng Zhuang*, Maurizio Burla, Caterina Taddei, Marcel Hoekman, Arne Leinse, Chris G.H. Roeloffzen, Klaus-J. Boller and Arthur J. Lowery

Programmable optical processor chips: toward photonic RF filters with DSP-level flexibility and MHz-band selectivity

https://doi.org/10.1515/nanoph-2017-0077
Received July 25, 2017; revised October 1, 2017; accepted October 30, 2017

Abstract: Integrated optical signal processors have been identified as a powerful engine for optical processing of microwave signals. They enable wideband and stable signal processing operations on miniaturized chips with ultimate control precision. As a promising application, such processors enables photonic implementations of reconfigurable radio frequency (RF) filters with wide design flexibility, large bandwidth, and high-frequency selectivity. This is a key technology for photonic-assisted RF front ends that opens a path to overcoming the bandwidth limitation of current digital electronics. Here, the recent progress of integrated optical signal processors for implementing such RF filters is reviewed. We highlight the use of a low-loss, high-index-contrast stoichiometric silicon nitride waveguide which promises to serve as a practical material platform for realizing high-performance optical signal processors and points toward photonic RF filters with digital signal processing (DSP)-level flexibility, hundreds-GHz bandwidth, MHz-band frequency selectivity, and full system integration on a chip scale.

***Corresponding author: Leimeng Zhuang,** Electro-Photonics Laboratory, Department of Electrical and Computer Systems Engineering, Monash University, Clayton, VIC 3800, Australia, e-mail: leimeng.zhuang@ieee.org. http://orcid.org/0000-0002-6948-5304
Yiwei Xie, Zihan Geng and Arthur J. Lowery: Electro-Photonics Laboratory, Department of Electrical and Computer Systems Engineering, Monash University, Clayton, VIC 3800, Australia
Maurizio Burla: Institute of Electromagnetic Fields (IEF), ETH Zurich, 8092 Zurich, Switzerland
Caterina Taddei and Klaus-J. Boller: Laser Physics and Nonlinear Optics Group, University of Twente, Enschede 7500AE, The Netherlands
Marcel Hoekman, Arne Leinse and Chris G.H. Roeloffzen: LioniX International, Enschede 7500AL, The Netherlands

Keywords: integrated microwave photonics; microwave photonic filter; photonic integrated circuit; waveguide; photonic RF filter; integrated optics.

1 Introduction

Radio frequency (RF) filtering is an essential analog processing function in RF communication and radar system front ends. Developing low-cost and flexible RF front ends is of high interest for both academia and industry [1], driven by the rapid and incessant increase of demand for data traffic in wireless communications for the consumer market [2], for example, the next-generation 5G systems, and high-frequency applications for defense and space industries [3]. Alongside the conventional all-electronics solutions that are supported by high industrial maturity but facing general challenges of bandwidth, tunability, and power consumption, microwave photonics offers practical solutions with desirable features such as large instantaneous bandwidth, low electromagnetic interference, wide continuous tunability, and high power efficiency [4–7]. In particular, these features benefit multi-gigahertz applications, for example, 60-GHz or W-band systems [8]. Implementing signal processing functions on photonic integrated circuits (PICs) [9–11] yields the so-called processing core chips with coveted practical features such as miniaturized size, long-term stability, ultimate control precision, reduced electromagnetic interference, and potential for low cost. Microwave photonic implementations of RF filters using integrated optical signal processors harvest all the features and advantages as mentioned above. In addition, they can be designed as “plug-in” components in analog optical links, expanding functions for radio-over-fiber technologies [12].

From a practical perspective, a major challenge for implementing such RF filters is the provision of a photonic integrated circuit technology platform that allows for simultaneous low loss, high compactness, an easy tuning

Open Access. © 2017 Leimeng Zhuang et al., published by De Gruyter. BY-NC-ND This work is licensed under the Creative Commons Attribution-NonCommercial-NoDerivatives 4.0 License.

mechanism, and viability for chip-scale integration of both active and passive functions. All these aspects are essential for the filter performance. Chip-scale integration effectively addresses the system stability issues. Low waveguide propagation loss is a dictating performance factor as signal path lengths in the order of centimeters or longer will be required for the feature of high-frequency selectivity (e.g. sub-GHz).

To date, a number of waveguide materials have been investigated for PICs including silicon-based materials [13–19], III–V semiconductors [20–22], $LiNbO_3$ [23], polymers [24, 25], chalcogenide glass [26], and metallic materials for plasmonic waveguides [27]. Either alone or combined, these materials, each with unique features, have enabled a wide diversity of passive and active functions, utilizing both linear and nonlinear optical properties. Some frequently shown examples include couplers, filters, (de)multiplexers, delay lines, lasers, amplifiers, modulators, detectors, phase conjugators, and wavelength convertors [10, 17, 20]. Although showing a great range of functions, implementing RF signal processing in microwave photonics may require a complex optical system that comprises a combination of many of these functions. In a broad sense, integrating such systems on monolithic chips [28, 29] or by means of micro-assembly of multiple chips [30–33] is a key for the proliferation of their large-scale application in real-world systems. To that scope, we need to simultaneously address the issues of device size, power consumption, and performance stability, as compared with all-electronics solutions [34]. Promisingly, recent rapid advances of high-index-contrast waveguides, that is, silicon-on-insulator (SOI), silicon nitride (Si_3N_4), and indium phosphide (InP), have successfully yielded many functions as standard building blocks for creating compact high-performance PICs. Besides, the constant improvement of fabrication maturity points toward large-scale integration of thousands of these functions with high-performance uniformity and repeatability [35–37].

In practice, the new PIC development model, that is, the fabrication paradigm of a generic foundry and business model based on multi-project-wafer runs (www.jeppix.eu), is expected to transfer the successful experience in the microelectronics industry to photonics and thereby give rise to an effective and efficient boost of PIC technologies to commercially viable solutions. One reason for this is that the fabrication time and cost efficiencies are largely increased by allowing multiple different functions to share the same fabrication process instead of each one requiring an independent process. Second, the lowered cost through wafer sharing enables cost-sensitive units such as university research groups and small-sized companies to get access to the state-of-the-art fabrication facilities as well as foundry-owned intellectual properties such as design methods and well-developed components as standard building blocks.

While the current PIC development is on a global scale, widespread commercial adoption of PIC devices in existing and prospect RF applications still requires a cost level comparable with microelectronics. This implies the need of a compelling market drive which allows for optimization of high-volume large-scale fabrication technology. However, most works of PIC prototyping for RF applications to date use the paradigm of application-specific PIC fabrication where a particular design of a PIC is made for a target function that often addresses only a potential for a niche market. One promising solution to this issue is the so-called programmable optical chip, in a similar concept of field-programmable gate arrays (FPGAs) and programmable processors in microelectronics, where functional programmability is incorporated in PICs so that a single device is able to implement multiple functions by means of software programming. This eventually means a hardware platform being able to serve a wide range of applications and thereby largely increasing the potential market and reducing the unit cost.

Here, we review recent progress of integrated optical signal processors for implementing RF filters with large bandwidth, continuous tunability, and shape reconfigurability. We highlight the use of a low-loss, high-index-contrast stoichiometric silicon nitride (Si_3N_4/SiO_2) waveguide which promises to serve as a practical material platform [38] for realizing high-performance optical signal processors and points toward photonic RF filters with digital signal processing (DSP)-level flexibility, hundreds-GHz bandwidth, and MHz-band frequency selectivity. These works demonstrate an enabling technology that brings unprecedented features to RF filters, and the results pave the way to commercial adoption and proliferation of photonic solutions for RF engineering.

The remainder of the paper is organized as follows: Section 2 provides an overview of fundamentals of microwave photonic filters and discusses a number of signal processing techniques for filter synthesis; Section 3 describes the waveguide technology; Section 4 presents a number of implementation examples of RF filters using our integrated optical signal processors; Section 5 addresses the development of optical signal processors that are designed to enable special filter features in terms of bandwidth, frequency selectivity, and filter shape reconfigurability; Section 6 explains the concept of general-purpose optical signal processors; Section 7 gives a

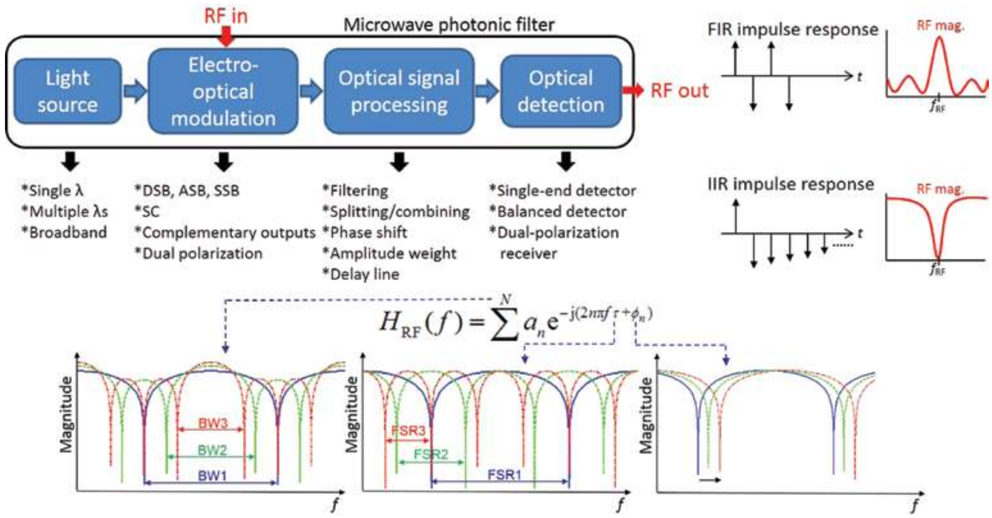

Figure 1: General system architecture of MWP filters.

general overview of the study of optical signal processors using other material platforms. Section 8 concludes this paper with our visions of future developments in this area.

2 Fundamentals of microwave photonic filter

2.1 System architecture

To date, a large number of microwave photonic implementations of RF filters have been demonstrated [39], utilizing various optoelectronic devices, linear and nonlinear optical properties in different materials, and manipulations of signal processing in all accessible domains of signal representation such as amplitude, phase, frequency, space, and polarization. Some salient works demonstrated remarkable filter features that outrun state-of-the-art all-electronics implementations, such as terahertz bandwidth [40], multi-octave tuning [41], nanosecond switching speed [42], microwatt control [43], and power extinction exceeding 60 dB [44]. Recent work of ours proposed and experimentally demonstrated a full-integration-ready approach of such filters with DSP-like flexibility by means of introducing software-defined circuit programmability into the processing core chips [45].

Figure 1 shows the general system architecture of microwave photonic filters. It comprises four basic functional parts: (i) light source, (ii) electro-optical modulation, (iii) optical signal processing, and (iv) optical detection. For the light source, coherent and incoherent light have been demonstrated, which include a single or multiple continuous wave (CW) lasers [39], frequency comb sources [46], and amplified spontaneous emission from erbium doped fiber amplifiers [47]. The recent advances of electro-optical modulators not only allow RF frequencies up to 100 GHz to be modulated on a lightwave, but also enable flexible configurations of modulated optical spectra such as double sidebands (DSB), asymmetric sidebands (ASB) [44], single sideband (SSB), optical carrier suppression (SC), dual polarizations, and simultaneous generation of two complementary outputs with opposite modulation phases. All these can be combined with a following optical signal processing stage to manipulate the amplitude and phase of different frequency components of the RF modulation sidebands in the optical domain. Eventually, optical detection, for example, using a single-end detector, a balanced detector, or a dual-polarization receiver, retrieves the RF output signal with the filtering effect synthesized in accordance with the manipulations in the optical signal processing. For the purpose of filter design, one can regard the entire operation as a “black-box”, where a combination of multiple optoelectronic devices are applied therein to implement equivalent RF systems described by particular impulse responses [48]. We confine our following discussion to tapped-delay-line-based interferometric filters characterized by discrete-time finite impulse response (FIR) and infinite impulse response (IIR). The synthesis of such filters is well described by digital filter theory and therefore enjoys the use of well-developed DSP algorithms for the design process. The general transfer functions of such filters can be formulated in the form of z-transform for digital filters:

$$H_{\mathrm{RF}}(z)=\sum a_n e^{-j\phi_n} z^{-n} \quad (1)$$

where a_n, ϕ_n, and z^{-n} represent the amplitude, phase, and index of the nth tap in the impulse response, respectively. The frequency response of the filter, $H_{\mathrm{RF}}(f)$, can be determined by evaluating Eq. (1) with $z^{-1}=e^{-j2\pi f\tau}$, where τ is the inter-tap delay and relates to the free spectral range (FSR) of the frequency response by $\tau=1/\Delta f_{\mathrm{FSR}}$. As illustrated in Figure 1, varying the tap coefficients in Eq. (1) reconfigures the filter shape, where generally the number of effective taps governs the frequency selectivity, inter-tap delay defines the frequency periodicity, and phase coordination determines the spectral positions of the filter passbands and stopbands.

2.2 Typical microwave photonic filter implementations

Figure 2 shows the typical approaches for microwave photonic filters that can be implemented using integrated optical signal processors. In general, one can divide them into incoherent filters and coherent filters [39]. For incoherent filters (Figure 2A), the generation of the filter impulse response does not require optical coherence between the taps. The FIR filters of this kind are commonly associated with a multi-λ light source or a broadband light source with an electrically or optically sliced spectrum [47, 49]. The impulse response taps are defined by wavelength or spectral slices, and the inter-tap delays are generated using either a dispersive medium or delay lines incorporated in a wavelength division multiplexing (WDM) architecture. In contrast, the IIR filters can be implemented by means of a combination of a single-λ light source with a frequency-shifting fiber-optical recirculating loop [50, 51]. Such filters are generally very flexible in terms of system configuration and also have possibilities of implementing tap coefficient tunability in the light source. On the other hand, however, they are often more challenging for photonic integration due to the use of a combination of system components in different materials.

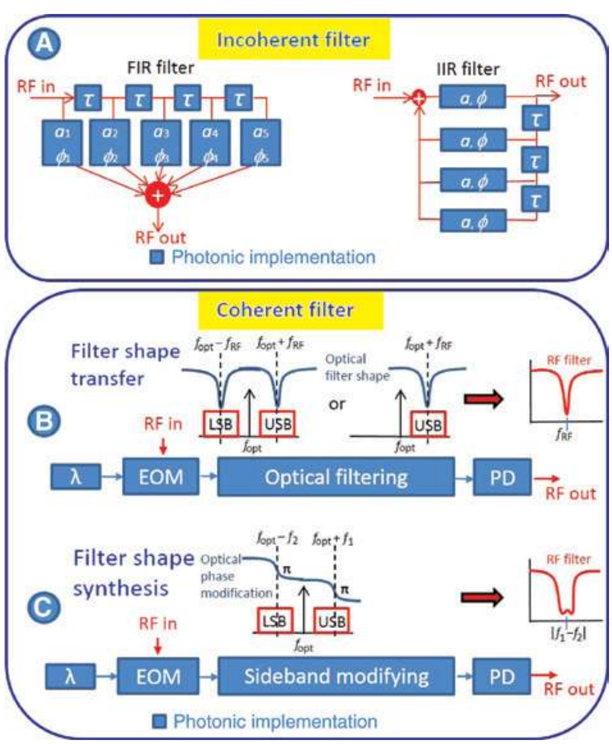

Figure 2: Typical approaches for implementing MWP filters. (A) Incoherent filter, (B) coherent filter by means of filter shape transfer, and (C) coherent filter by means of filter shape synthesis.

For coherent filters (Figure 2B and C), the so-called filter shape transfer and filter shape synthesis are two common approaches based on modifying the modulated optical spectrum via coherent processing in optical filters. In the former approach, the RF sidebands in the modulated optical spectrum are directly filtered by means of optical filters with the desired filter shape, and then optical detection results in a consistent transfer of this filter shape to the RF output. As illustrated in Figure 2B, both SSB and DSB modulation can be employed, with only DSB modulation requiring optical filtering to the two sidebands in a mirror-symmetric manner with respect to the optical carrier frequency [52]. In the latter approach, both sidebands are generated via DSB or ASB modulation and also pass through optical filters. However, in this case, the two sidebands are individually modified in terms of amplitude and phase. After optical detection, the two sidebands yield two modified copies of the input RF signal and the interference between them translates the amplitude and phase differences into a filter shape. Such coherent filters feature simple system configurations and therefore are more favorable for photonic integration.

3 TriPleX silicon nitride platform

3.1 Waveguide technology

Typically, waveguide filters working in the RF/microwave region employ delay lines with significant lengths. In particular, the feature of MHz-band frequency selectivity requires waveguide path lengths in the order of centimeters or longer. This means that low optical propagation loss is a key dictating factor for the filter performance. In general, low-index-contrast (<5%) waveguides such as phosphorus-doped silicon dioxide and silicon oxinitride are easy to be provided with low optical propagation losses, for example, <0.05 dB/cm [53]. However, such waveguides have strong limits on the minimum bend radius, which is typically in the order of millimeters. This is because significant radiation loss occurs for small bend radii due to the low mode confinement of the waveguide. This forces the footprints of the building blocks to be rather large, with the minimum bend radius in micrometer given by, as a rule of thumb, $R_{min} = 5\Delta n^{-1.5}$ for 0.1 dB/rad radiation loss [54].

Our development of integrated optical signal processors uses a stoichiometric Si_3N_4/SiO_2 waveguide technology (TriPleX™ waveguide technology, a proprietary technology of LioniX International) which features simultaneously low-loss, high-index-contrast, and complementary metal-oxide-semiconductor (CMOS) fabrication equipment compatibility [16]. Figure 3 shows the waveguide propagation losses measured in ring resonator (RR) circuits with different bend radii and negligible coupler excess loss (using adiabatic designs), where a very low systematic loss of 0.095 dB/cm is achieved for a bend radius of 70 μm [38]. The waveguide consists of two strips of Si_3N_4 with a thickness of 170 nm surrounded by SiO_2, as illustrated in the scanning electron microscope photograph in Figure 3. The use of this two-stripe geometry increases the effective index of the optical mode as compared to a single-stripe geometry. As a consequence, the mode confinement of the waveguide increases, which reduces the bend loss. The waveguide width is typically 1.2 μm at the top interface of the upper stripe, the intermediate SiO_2 layer between the stripes is 500 nm thick, and the side wall angle of the waveguide due to the etching process is between 80° and 82°. These dimensions are the result of an optimization that provides a high effective index of the mode while the waveguide only supports a single mode at a wavelength of 1550 nm. Besides, this waveguide geometry design was also chosen in order to match TriPleX production standards which increase device reproducibility. This waveguide is single-mode and has a thermal dependency of $dn_{eff}/dT = 4.1 \times 10^{-6}$ for both transverse-electric (TE) and transverse-magnetic (TM) polarization. Due to a birefringence of about 0.054 (1.535 for TE and 1.481 for TM), the TM mode is much less confined and therefore experiences much more loss in bend sections as compared to the TE mode. Hence, for low-loss applications, only TE polarization is considered, which corresponds to a theoretical group index of 1.708 at 1550 nm wavelength [16]. As depicted in Figure 3, in this waveguide, the Si_3N_4 is deposited using low-pressure chemical vapor deposition (LPCVD) and the SiO_2 includes three different types: wet thermally oxidized silicon substrates are used for the bottom SiO_2 layer of 8 μm; the middle SiO_2 layers are deposited using LPCVD; and the SiO_2 for the top cladding are fabricated using plasma-enhanced chemical vapor deposition.

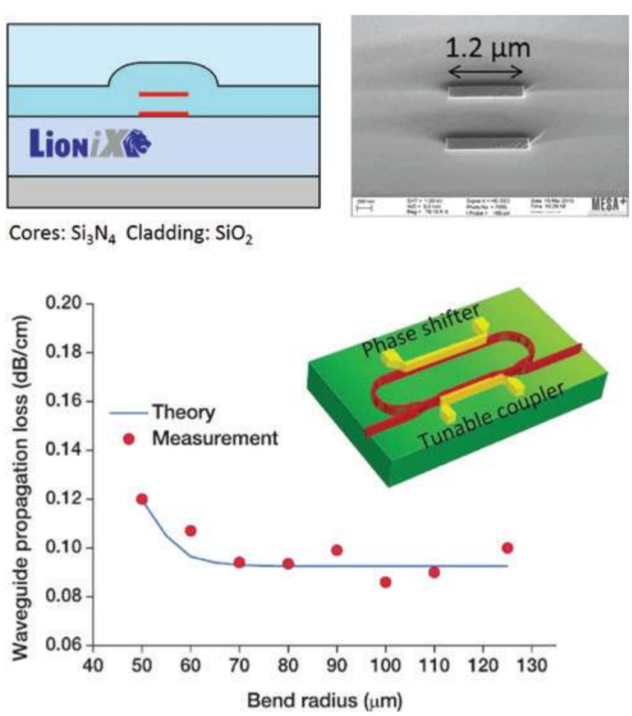

Figure 3: Schematic and scanning electron microscope photograph of the Si_3N_4/SiO_2 waveguide cross-section and the waveguide losses measured in ring resonators [38] (Copyright in 2010, Optical Society of America).

As shown in Figure 3, chromium heaters as tuning elements can be defined at the appropriate places on top of the top cladding to implement the thermo-optical phase tuning mechanism. At present, such a heater with a width of 20 μm and a length in the order of 2000 μm is able to operate at a switching speed of about 0.5 ms and a power efficiency of about 0.25 W/π. This heater width is easy to make with lift-off lithography and gives margin on the exact alignment of the heater above the waveguides. In principle, the resistance of a heater is determined by thickness and width, so heaters, for example, with a width of 10 μm but larger thickness can also be used. In practice, Mach-Zehnder interferometers (MZIs) with such heaters on their arms can be constructed as tunable couplers to implement optical amplitude control [10].

3.2 Basic processor building blocks

Figure 4 shows the schematics of basic waveguide building blocks for constructing integrated optical signal

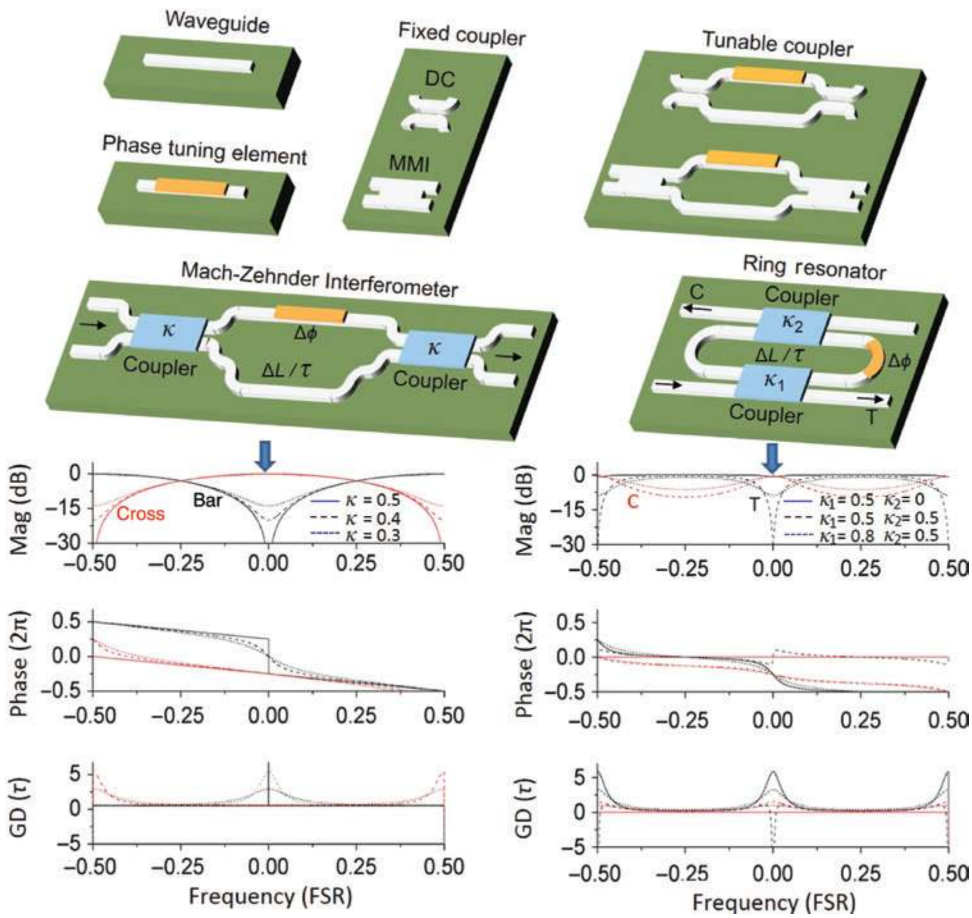

Figure 4: Schematics of basic waveguide building blocks for constructing integrated photonic signal processors and architectures as well as frequency responses examples of a Mach-Zehnder interferometer and a ring resonator (Mag, magnitude; GD, group delay).

processors. Delay lines can be implemented by using different lengths of waveguide. Splitting and combining can be implemented using directional couplers (DCs) or multi-mode interferometers. For interferometric filters, an asymmetric MZI or an RR that implements respectively first-order FIR and IIR filters can be constructed by using a combination of couplers and delay lines. Their transfer function matrices in z-transform can be formulated as

$$H_{\mathrm{AMZI}}(z)=\begin{bmatrix} -s^2\gamma_{\Delta L}z^{-1}+c^2\mathrm{e}^{-\mathrm{j}\phi} & -\mathrm{j}cs(\mathrm{e}^{-\mathrm{j}\phi}+\gamma_{\Delta L}z^{-1}) \\ -\mathrm{j}cs(\mathrm{e}^{-\mathrm{j}\phi}+\gamma_{\Delta L}z^{-1}) & s^2\gamma_{\Delta L}z^{-1}-c^2\mathrm{e}^{-\mathrm{j}\phi} \end{bmatrix} \tag{2}$$

and

$$H_{\mathrm{RR}}^{\mathrm{T}}(z)=\frac{c_1-c_2\gamma_{\Delta L}z^{-1}\mathrm{e}^{-\mathrm{j}\phi}}{1-c_1c_2\gamma_{\Delta L}z^{-1}\mathrm{e}^{-\mathrm{j}\phi}},H_{\mathrm{RR}}^{\mathrm{C}}(z)=\frac{-s_1s_2\sqrt{\gamma_{\Delta L}z^{-1}\mathrm{e}^{-\mathrm{j}\phi}}}{1-c_1c_2\gamma_{\Delta L}z^{-1}\mathrm{e}^{-\mathrm{j}\phi}} \tag{3}$$

where $c=\sqrt{1-k}$ and $s=\sqrt{(k)}$ are the field coupling coefficients, and γ is the amplitude factor determined by the waveguide loss (assuming that the adiabatic design of the couplers gives negligible excess loss and its effect can be left out). Some examples of their frequency responses are shown in Figure 4. Based on these functions, one can design higher order filters and other more complex functions such as switch networks [45] and multiplexers [55] by combining a number of these basic building blocks. For the filter control, a manipulation of the tap coefficients can be implemented using the circuit parameter, that is, phase and amplitude, tuning mechanisms supported by the waveguide technology.

4 Examples of microwave photonic filters

4.1 Incoherent filters

RRs are very versatile devices in terms of signal-processing functions. Next to the delay line function, the phase response of an RR can be configured with a sharp phase variation slope and a slope with a phase deviation range of 2π can be generated by properly configuring a serial cascade of two or more RRs [48]. For a multi-λ incoherent filter, this function in association with SSB modulation can be applied to perform separate optical carrier phase control and thereby provide complex coefficient to the filter taps. With this principle, a work of ours demonstrated an integrated optical signal processor comprising tunable delay lines, separate optical carrier phase control, and an optical sideband filter using a ring resonator-assisted Mach-Zehnder interferometer (RAMZI) in one unit [56], as illustrated in Figure 5. With this processor, two-tap incoherent filters have been successfully demonstrated, where both the notch frequency and FSR can be fully adjusted over a bandwidth of 1 GHz. The result of this work shows the function variety of the silicon nitride platform in use and, more importantly, the possibility of realizing fully integrated microwave photonic filters.

4.2 Coherent filters

Although RF electronics are well developed and are supported by mature fabrication technology and industry, there are still technology gaps in RF filters. Specifically, it is very challenging to provide large tuning ranges (multiple octaves) at high frequencies (e.g. >20 GHz) in a compact device. RF filters with these features are highly desired in many wideband, frequency-agile systems such as radar and cognitive radio communications [57, 58], where a breakthrough of filter performance would lead to a significant improvement of the existing systems or the possibility of enabling new system functions. Integrated microwave photonic filters open an alternative path for this purpose, enjoying intrinsic advantages in terms of bandwidth, tunability, and size. In particular, coherent IIR filters are able to be designed to provide very high frequency selectivity [59].

Typical waveguide implementations of IIR filters are coupled with RRs and RAMZIs [48]. For the integrated microwave photonic implementation of coherent filters, both approaches in Figure 2, that is, filter shape transfer and filter shape synthesis, have been demonstrated. As a salient example for such a filter shape transfer approach, Rasras et al. [52] demonstrated an RF notch filter using an RAMZI comprising a four-ring resonator-assisted symmetric MZI with a total chip area of 1.75 mm^2 and an RR FSR of 43 GHz. This work demonstrated a notch depth >30 dB, a 3-dB bandwidth <1 GHz, a tuning range >15 GHz, and the capability of multiple notches at the same time.

With the filter shape synthesis approach, RF filters with even more distinct features have been demonstrated. Palací et al. [60] demonstrated an RF bandpass filter featuring a very simple system configuration. The filter comprises a serial connection of a CW laser, a phase modulator, a silicon RR, and a photodetector. In the working principle, as illustrated in Figure 2, the resonance frequency of the RR with an FSR of about 500 GHz is aligned to one of the RF-modulated sidebands which introduce differences of amplitude and phase between the two sidebands for a certain bandwidth. After optical detection, the RF frequencies within the bandwidth are passed while those outside are suppressed. In the result, a filter bandwidth of about 8.5 GHz and a frequency tuning range of about 100 GHz were shown. Most importantly, the experimental demonstration in this work predicted the possibility of implementing such filters with frequency selectivity in the MHz level and the proven filter shape synthesis principle inspired many later works.

In a further exploration, Marpaung et al. demonstrated an RF notch filter using a Si_3N_4 RR with a similar system complexity [61]. The filter features a very deep notch extinction of about 60 dB, showing an advantage of microwave photonics over conventional all-electronics RF filters. The implementation of the notch filter is shown in Figure 6, where an asymmetric configuration of sidebands in the modulated optical spectrum is used. The RR's resonance frequency is aligned to the stronger sideband and is configured such that the filtered area in the stronger sideband has a residual portion with equal amplitude and π-phase difference with respect to the weaker sideband. After optical detection, this particular optical spectrum modification results in a nearly complete power cancellation at the resonance-filtered frequency. Using an RR with an FSR of 20 GHz, a filter 3-dB bandwidth <400 MHz, and an RF frequency tuning range of 8 GHz were successfully demonstrated. As the RR's FSR in principle covers both RF sidebands of the modulated optical spectrum, an FSR larger than twice the desired RF tuning range should be used in such implementations. In a further investigation of this filter approach, Liu et al. [62] incorporated stimulated Brillouin scattering gain in fiber into the processing system and thereby implemented a lossless RF notch filter with high-frequency resolution.

4.3 Reconfigurable filters

From a filter implementation point of view, next to the filter performance, filter shape reconfigurability is another key challenge for the filter design as it significantly broadens

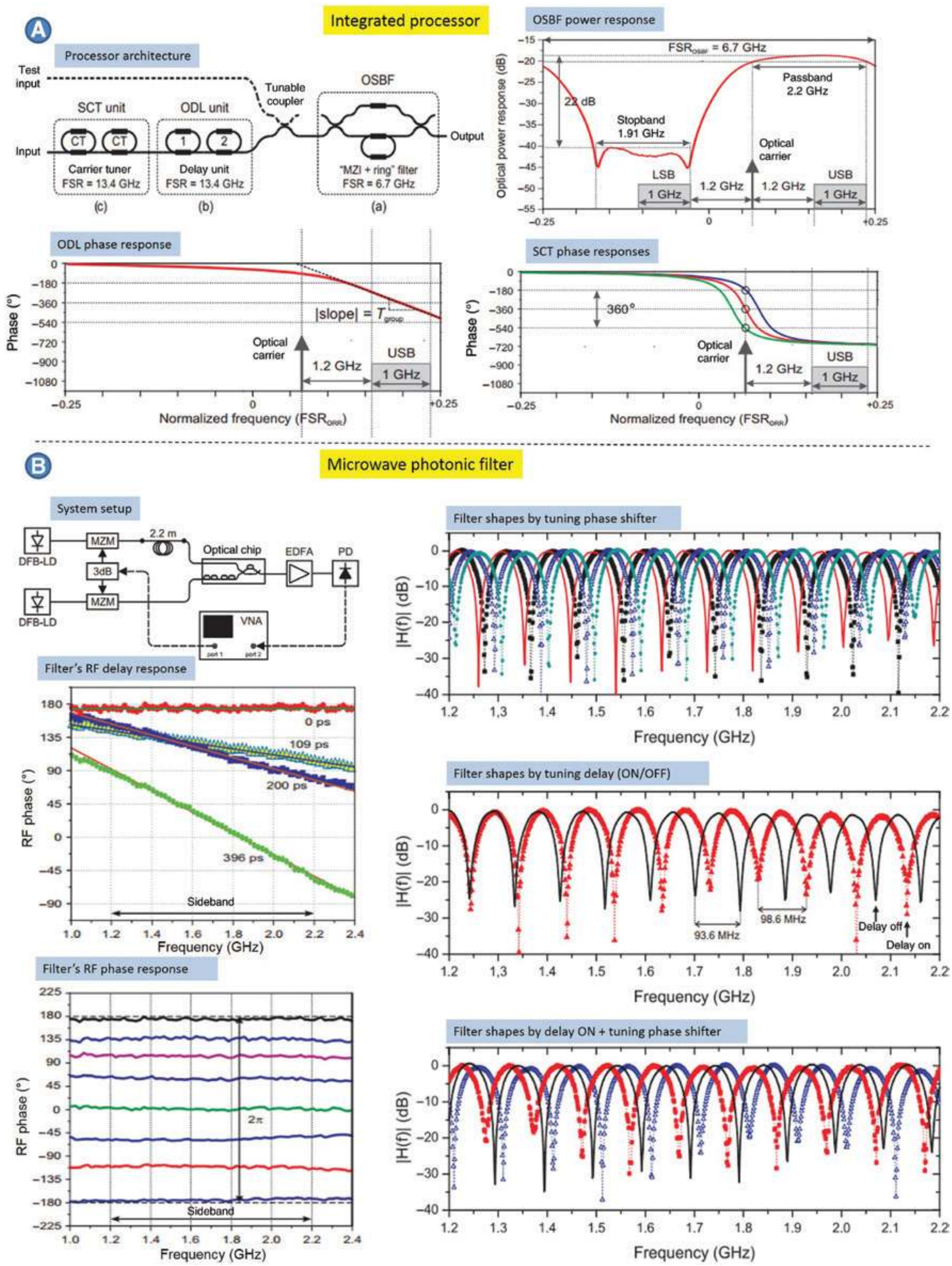

Figure 5: An integrated optical signal processor and a microwave photonic filter.
(A) An integrated photonic signal processor design comprising tunable delay lines, separate carrier tuning, and an optical sideband filter.
(B) An implementation of a two-tap microwave photonic filter [56] (Copyright in 2011, Optical Society of America).

the potential for application of a filter. Considering such filters as industrial products, a wide application range is an important incentive for volume production, which is the most effective path for optimizing the filter performance and reducing the fabrication cost. Motivated by this challenge, we further explored the utilization of optical spectrum modification and proposed a highly reconfigurable RF filter implemented using an integrated processor chip

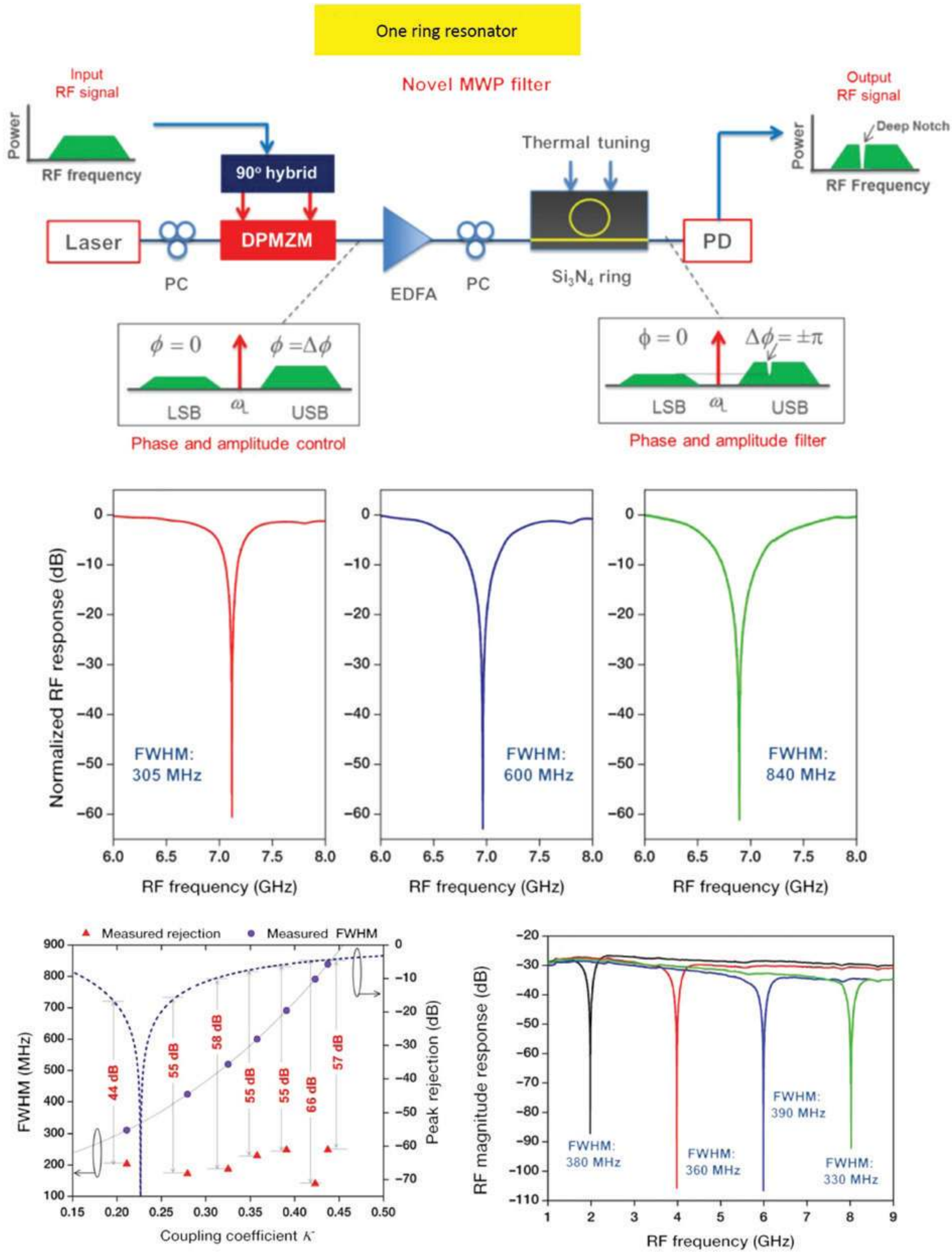

Figure 6: Microwave photonics implementations of RF filters using optical signal processor chips that comprise one ring resonators, showing the evolution toward DSP flexibility [61] (Copyright in 2013, Optical Society of America).

comprising a serial cascade of a pair of silicon nitride RRs [45]. In the experimental demonstration, DSB modulation is employed, which can be easily implemented using an intensity or phase modulator. Two RRs are configured such that each has its resonance frequency aligned to one of the sidebands as illustrated in Figure 7. Owing to the use of two RRs, a new degree of freedom is introduced to the spectrum modification, which enables the two sidebands to be modified independently of each other. After optical detection, a variety of filter shapes can be synthesized, as shown in Figure 7. Using a pair of RRs with an FSR of 14 GHz, a filter frequency tuning range greater than two octaves, that is, from 1.6 to 6 GHz, and variable filter shapes ranging from a 55-dB extinction notch filter to a bandwidth adjustable flat-top bandpass filter were successfully demonstrated. While this result proves the possibility of implementing multiple different RF filter shapes using one simple microwave photonic system, the operation of switching between bandpass filters and bandstop filters requires a separate optical carrier phase change which, in this case, must be performed off the processor chip and thereby left an open problem for processor chip design for the purpose of full system integration.

Having a whole microwave photonic filter system on a fully integrated unit provides the ultimate system stability, control precision, and device compactness. These aspects often play the dictating roles for practical RF filter implementations, particularly for airborne and spaceborne applications. Toward this goal, we proposed a particular processor design that comprises a serial cascade of three RRs of different FSRs [63], as illustrated in Figure 8. In this design, again, a pair of RRs with identical FSRs are used for filter shape synthesis and a third RR with a smaller FSR is used to perform the function as a modulation translator [64, 65] that enables a separate manipulation of the optical carrier phase. This processor works with DSB modulation and allows for the use of a simple phase modulator. In the experimental demonstration, an RF filter with a nearly DSP-flexible shape reconfigurability was demonstrated using such a processor fabricated in silicon nitride. This means that all the reconfiguration operations including filter frequency tuning, bandwidth variation, and switching between bandpass and bandstop filter shapes are implemented using the tuning mechanism on the processor chip, for example, DC-voltage-driven resistor heaters in this case. For one thing, this processor

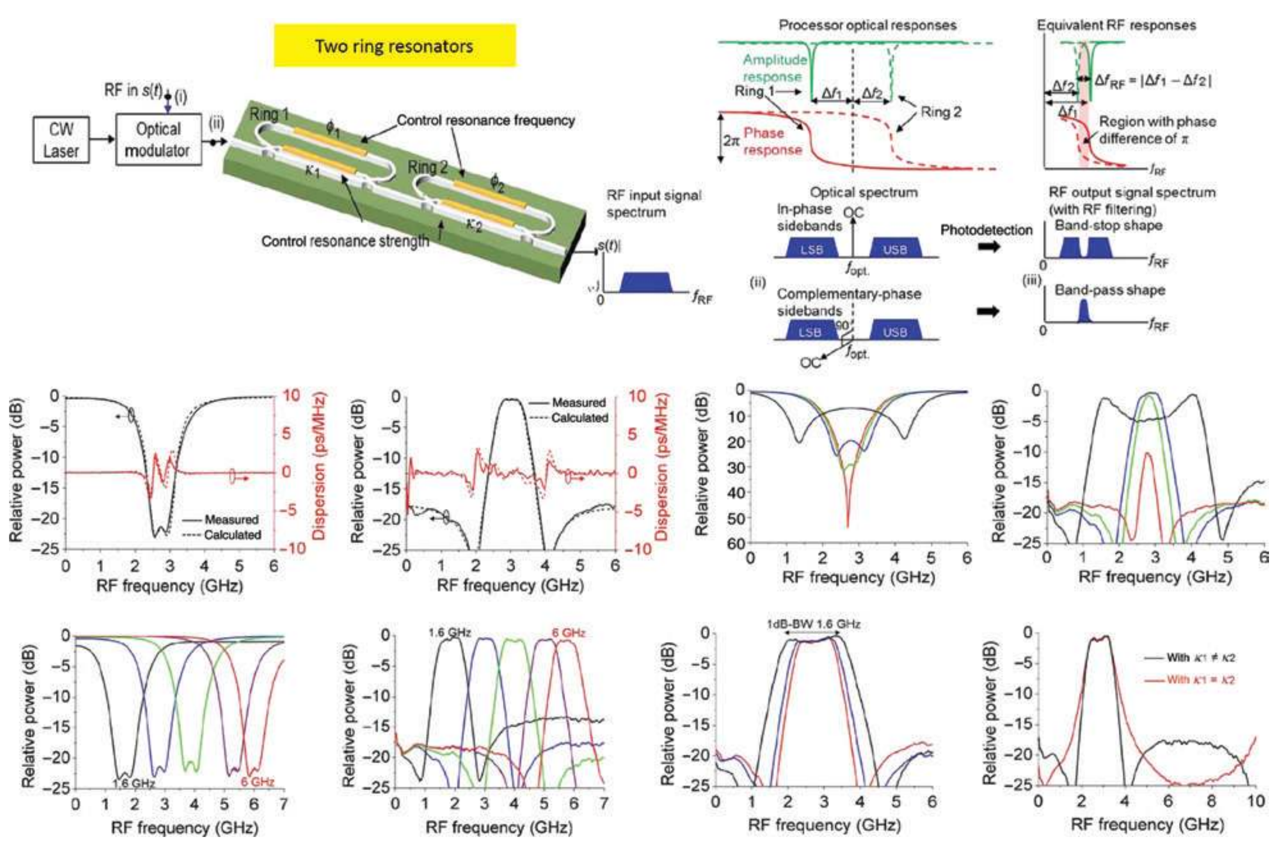

Figure 7: Microwave photonics implementations of RF filters using optical signal processor chips that comprise two ring resonators, showing the evolution toward DSP flexibility [45] (Copyright in 2015, Optical Society of America).

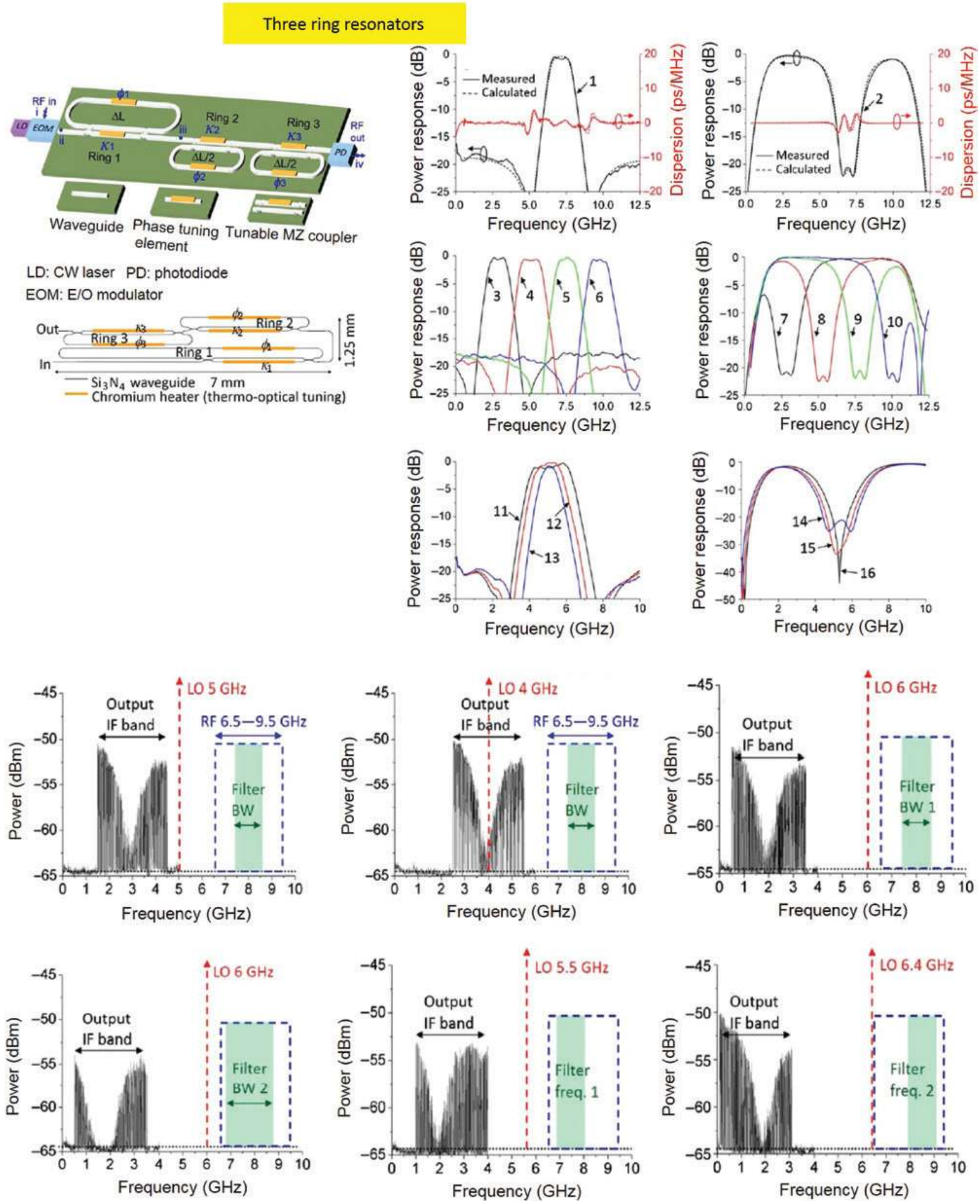

Figure 8: Microwave photonics implementations of RF filters using optical signal processor chips that comprise three ring resonators, showing the evolution toward DSP flexibility and incorporation of frequency down-conversion [63] (Copyright in 2016, Optical Society of America).

capability minimizes the function requirements of the remaining components in the system, that is, a CW laser, a phase modulator, and a photodetector, which benefits the system in terms of reduced complexity. More importantly, this system configuration is in favor of full system integration in one unit via the TriPleX-InP hybrid integration. While this particular reconfigurable RF filter has not been demonstrated in such a hybrid integration on the full scale, other parallel works have successfully demonstrated a unit based on the integration of a similar silicon nitride processor chip and an InP chip that provides active components [32]. These works will be discussed further in Section 5. In addition, the filter approach in Figure 8 also allows for a simultaneous implementation of the RF frequency down-conversion function which is an essential function for RF front ends. This implementation employs a dual-parallel Mach-Zehnder modulator performing DSB-SC modulation where one sub-MZM is driven by the RF signal and the other sub-MZM is driven by an RF local oscillator. These two RF signals will pass the RRs together as two frequency components in the modulated optical spectrum and then mix with each other at photodetector. In the scenarios of photonics-assisted RF front ends, this implementation avoids the use of electrical mixers and allows for frequency mixing over the entire modulator bandwidth (typically >20 GHz). This feature is important for wideband RF systems and enables higher flexibility for frequency designs of RF front ends.

5 Essentials of optical signal processors

5.1 Tunable delay lines

Tunable delay lines play a key role in the implementation of optical signal processors. Broadband and highly selective filters typically require delays in the order of nanoseconds over bandwidths of tens of GHz. It is a great challenge to implement such delays using a length of waveguide on chip due to the limited physical chip area. However, several recent works of ours proposed possible solutions for tunable on-chip delay lines and demonstrated promising results. Our solution uses RRs comprising tunable phase shifts in the ring loops and tunable couplers. In principle, an RR can be configured to be an optical all-pass filter [48]. Its group delay at the resonance frequency can be set to be much larger than the round-trip delay of the ring loop and can be controlled via the coupler. This enables us to realize long delays using a small chip area. Besides, subject to the linear system principle, one can connect multiple RRs in a serial cascade to implement delay addition or delay bandwidth enlargement by means of manipulating the RRs' resonance frequencies. A schematic with six different configuration examples is shown in Figure 9. We have successfully demonstrated the use of such tunable delay lines in integrated optical beamforming network circuits for K_u-band satellite tracking phased array receivers [67], where a maximum delay of 1.2 ns with a bandwidth of 2.5 GHz was implemented using a serial cascade of seven RRs.

The conventional delay lines on the left of Figure 9 use identical RRs, which have a delay response that is periodic with frequency. This means that when used for multi-λ-based incoherent FIR filters, in general, each λ will require an independent delay line to generate the different delays of the filter taps. This gives rise to circuit complexity issues for filters with a large number of taps. An alternative approach to address this issue is to create delay lines that are able to simultaneously provide multiple different delays at different wavelengths or optical carrier frequencies. We proposed and experimentally demonstrated such delay lines using the Vernier configurations of RRs [66], namely combining RRs of different FSRs. Two types of Vernier configurations were considered as shown in Figure 9, that is, the serial cascade and coupled configurations, where the former features easier control and the latter less chip area. The core concept here is to implement multiple different delays staggered in frequency. In principle, a combination of RRs with N different FSRs allow for the simultaneous generation of $2^N - 1$ different delays per frequency period. This can be employed in multi-λ schemes of incoherent filters to significantly reduce the system complexity. As shown on the right of Figure 9, an inter-delay step of 550 ps and a maximum delay of 1650 ps for a bandwidth of 500 MHz were achieved using four-ring Vernier configurations of RRs with FSRs of 16 and 24 GHz.

5.2 MHz-band frequency selectivity

Satellite communications is one of the most interesting application areas for integrated microwave photonics technologies as size, weight, and power consumption are the key aspects of spaceborne or airborne RF devices regarding construction and operation costs [68]. For microwave photonic solutions to the traditional RF functions in this area such as RF filters and beamformers for phased array antennas [69–73], optical filters that

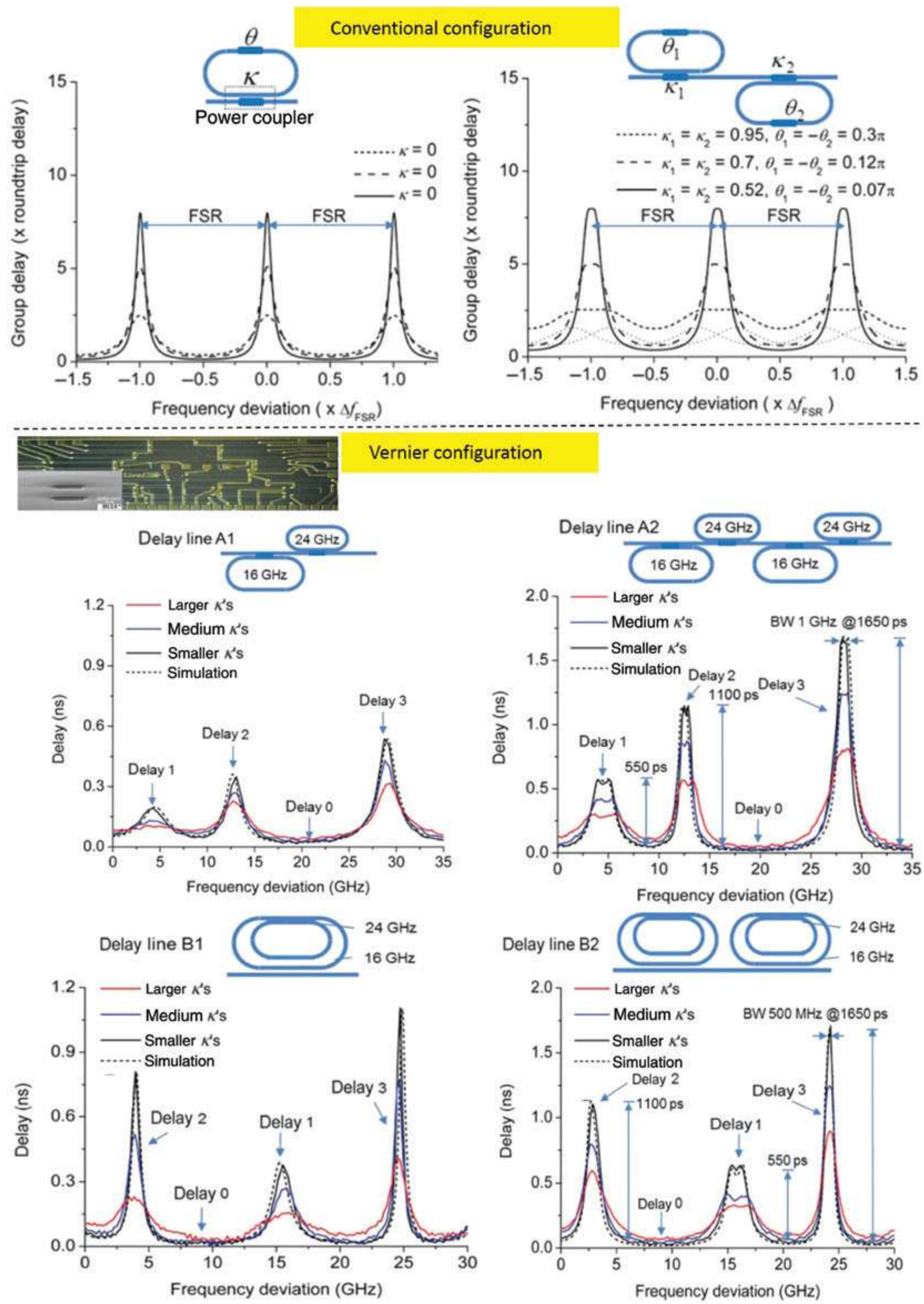

Figure 9: Tunable delay lines implemented using conventional and Vernier configurations of ring resonators [66] (Copyright in 2013, Wiley).

are able to provide MHz-band frequency selectivity can play an enabling role in satisfying the standard system requirements. One potential application of high interest is RF filters for input and output multiplexers (IMUXs and OMUXs) of satellite transponders that currently rely on bulk electronics. For example, a Ku-band OMUX requires a channel bandwidth ranging from 27 to 95 MHz for the frequency band from 10.7 to 12.75 GHz (www.thalesgroup.

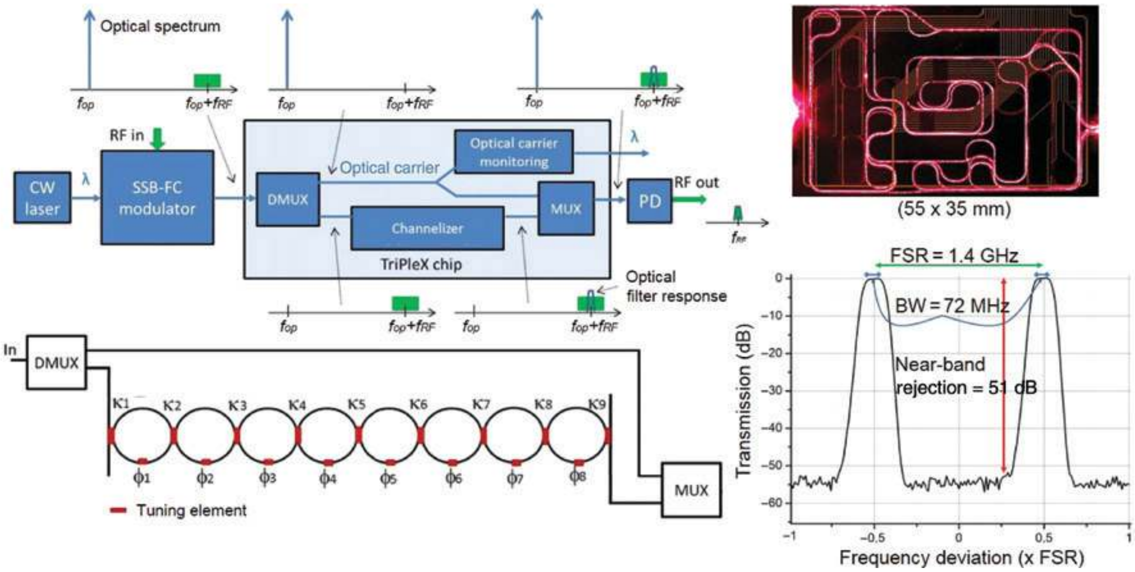

Figure 10: Design and realization of an on-chip optical filter for microwave photonic implementation of an RF bandpass filter with a bandwidth of 72 MHz [74] (Copyright in 2014, MWP/APMP).

com). Such RF filter requirements raise a great challenge for the design and fabrication of optical filters for microwave photonic implementations. As a promising technology, TriPleX silicon nitride waveguides offer a possible path to realize optical filters satisfying such requirements. We designed and fabricated a processor chip comprising an optical carrier-sideband demultiplexer and a multiplexer with a highly frequency-selective optical filter in between [74]. Here, a filter shape transfer approach employing SSB modulation is considered as illustrated in Figure 10. The optical filter is an eighth-order coupled RR network with an FSR of 1.4 GHz and has tunable couplers and tunable phase shifters in all ring loops. By properly configuring these tuning elements, a remarkable filter performance was experimentally demonstrated, that is, a 3-dB passband of 72 MHz, a –30-dB bandwidth of about 140 MHz, and a stopband rejection of 51 dB, while maintaining a very low filter insertion loss (excluding fiber-chip coupling losses) of <6 dB. As an important milestone of the waveguide technology, this filter shows an excellent combination of frequency selectivity, power rejection, and insertion loss when using the longest waveguides that were ever applied in such filters, that is, each ring loop having a length of 143 mm. This sets up a new benchmark for waveguide realizations of optical filters operating in the RF/microwave region, all thanks to the very low propagation loss, dispersion, as well as nonlinearity of the silicon nitride waveguide and excellent fabrication uniformity. In addition, the incorporation of the tuning elements allows for effective compensation for possible fabrication tolerances, and also enables filter shape reconfigurability that provides great potential for a wide range of applications.

Yu et al. [75] recently presented another design of a highly selective filter in TriPleX, using a serial cascade of three MZIs with different inter-arm delays as shown in Figure 11. This design allows for easy configuration of the filter passband as each MZI can be controlled independently. In the experiment, a fabricated filter showed a passband bandwidth of 143 MHz for an FSR of 1.466 GHz. When used in serial cascade with a second stage filter with a larger FSR, a high-frequency-contrast signal channelizer was achieved which features a frequency resolution of 143 MHz and an operation range of 112.5 GHz. An application example of this function in a frequency down-converted receiver proved its promising use for signal extraction in photonics-assisted RF front ends operating from L-band to K-band.

5.3 Circuit topology reconfigurability

For microwave photonic implementation of an RF filter using an optical filter on an integrated optical signal processor, the RF reconfigurability of the filter relies mostly on the optical reconfigurability. In the processor design, using tuning elements to enable the tunability of all possible circuit parameters maximizes the reconfigurability. A representative design in our previous works is an RAMZI circuit which comprises an asymmetric MZI with

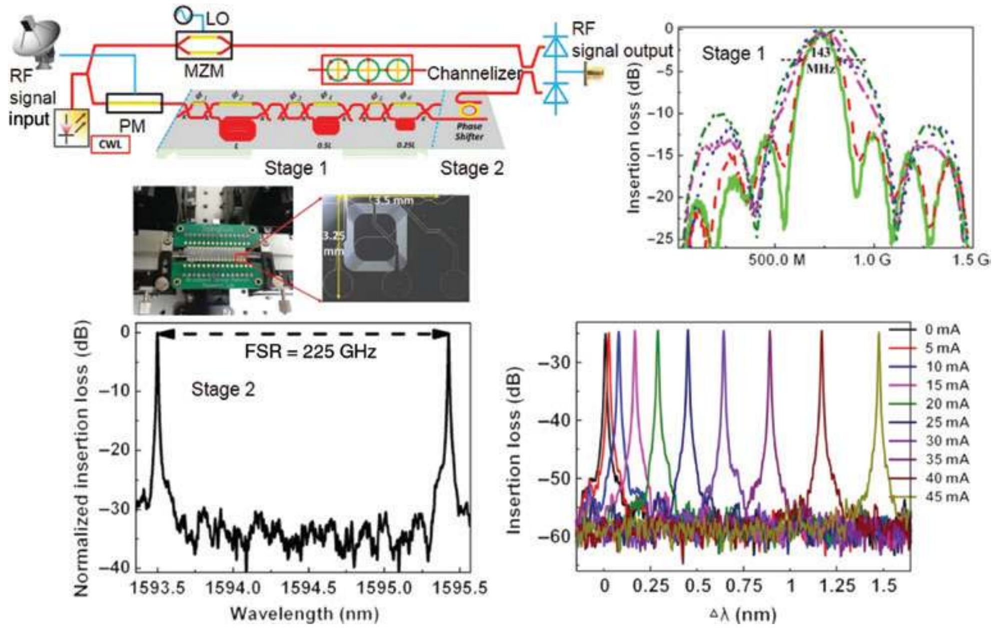

Figure 11: Design and realization of a highly selective signal channelizer featuring a frequency resolution of 143 MHz and an operation range of 112.5 GHz [75] (Copyright in 2015, IEEE).

each arm coupled with an RR as shown in Figure 12. The circuit employs a total of seven tuning elements, that is, two tunable couplers at the input and output of the MZI, two tunable couplers of the two RRs, and three tunable phase shifters in the ring loops and MZI delay line, all implemented using the resistor-based heaters as illustrated in Figure 3. As a reconfigurable processor, this common circuit design enabled a variety of different implementations of optical filters as shown in Figure 12. We configured the circuit into only an asymmetric MZI with both of the RRs decoupled off the MZI (by setting the tunable couplers of the RRs to zero coupling), and therewith demonstrated a notch filter [76]. It is also able to perform an optical sideband filter for the RF-modulated optical spectrum [38], where two different filter passband roll-offs were performed by means of having only one or both RRs coupled with the MZI and having all parameters of couplers and phase shifters properly set. In further work, using the same two-ring-coupled circuit configuration but a different setting of the phase shifters, we demonstrated an implementation of a narrow bandpass filter [77].

When provided with circuit topology reconfigurability, integrated optical signal processors possess a great potential for a wide range of practical applications, reaching into many areas in RF and optical engineering. Taking an RAMZI as an example, to date a number of its applications have been demonstrated beyond RF filters. One application is a wideband RF splitter which supports arbitrary amplitude, phase, and delay offsets [78]. Here, the two complementary outputs of the RAMZI were used to separate the two modulation sidebands and thereby yield two copies of the RF signal. In another work, an RAMZI is used for a photonic implementation of a wideband RF polarization network for dual-polarization linear antennas [79]. In this case, as shown in Figure 13, the RAMZI has its MZI configured to be two parallel tunable RF phase shifters that manipulate the radiation of wideband antennas between linear and circular polarizations. Another interesting use of an RAMZI, which has been well discussed for WDM systems in fiber communication networks, is the function as a frequency (de)interleaver [80]. When properly designed, the interleaver passband is also able to spectrally shape a transmission channel to nearly Nyquist bandwidth, that is, performing the function as a Nyquist-filtering interleaver. This function is of great interest for multiplexing and demultiplexing of WDM superchannels that have sub-channel spacings much smaller than the standard WDM grids (i.e. 50 and 100 GHz), and thereby opens a path toward the realization of WDM superchannel reconfigurable optical add-drop multiplexers (ROADMs). This technology is of great use for the implementation of next-generation elastic communication networks [81] that are aimed to provide unprecedented spectral efficiencies. We experimentally demonstrated

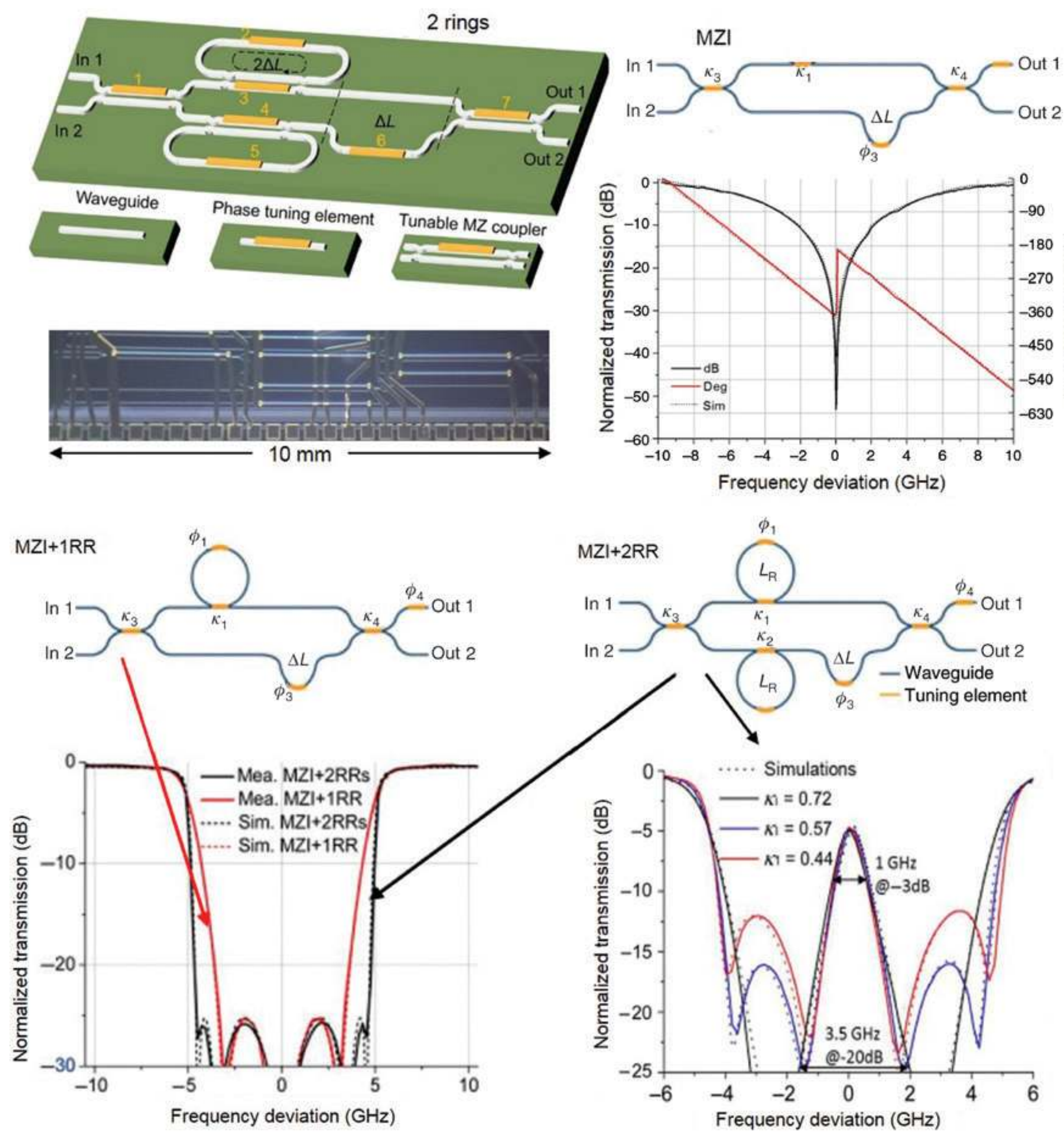

Figure 12: Design and realization of a highly reconfigurable RAMZI circuit: implementations of various optical filters using a regular RAMZI [76, 77] (Copyright in 2013, MWP, Copyright in 2014, IEEE).

this concept [55]. Two experiments addressing the multiplexing and demultiplexing functions were performed using an RAMZI with an interleaver period (FSR) of 25 GHz and a 3-dB passband bandwidth of 12.5 GHz as shown in Figure 14. In one experiment, the generation of a 7 × 12.5 Gbaud WDM superchannel was demonstrated with the RAMZI working as a Nyquist-filtering interleaver. Here, both CW lasers and periodic optical pulse trains can be used as the light source. In the other experiment, the RAMZI is used as a pre-deinterleaving stage in combination with a commercial wavelength-selective switch (WSS) to implement a resolution-enhanced WSS. Using this combination, a WDM superchannel ROADM was enabled, which supports a sub-channel spacing of 12.5 GHz, a factor of 4 smaller than the standard 50-GHz WDM grid. In further work, we investigated an RAMZI with different design variations, for example, narrowing the passband roll-off by increasing the number of RRs and expanding a two-port interleaver into an *N*-port multiplexer by merging an RAMZI with a circuit that performs the Fourier transform [82, 83]. The applications of these new variations are expected to further improve the

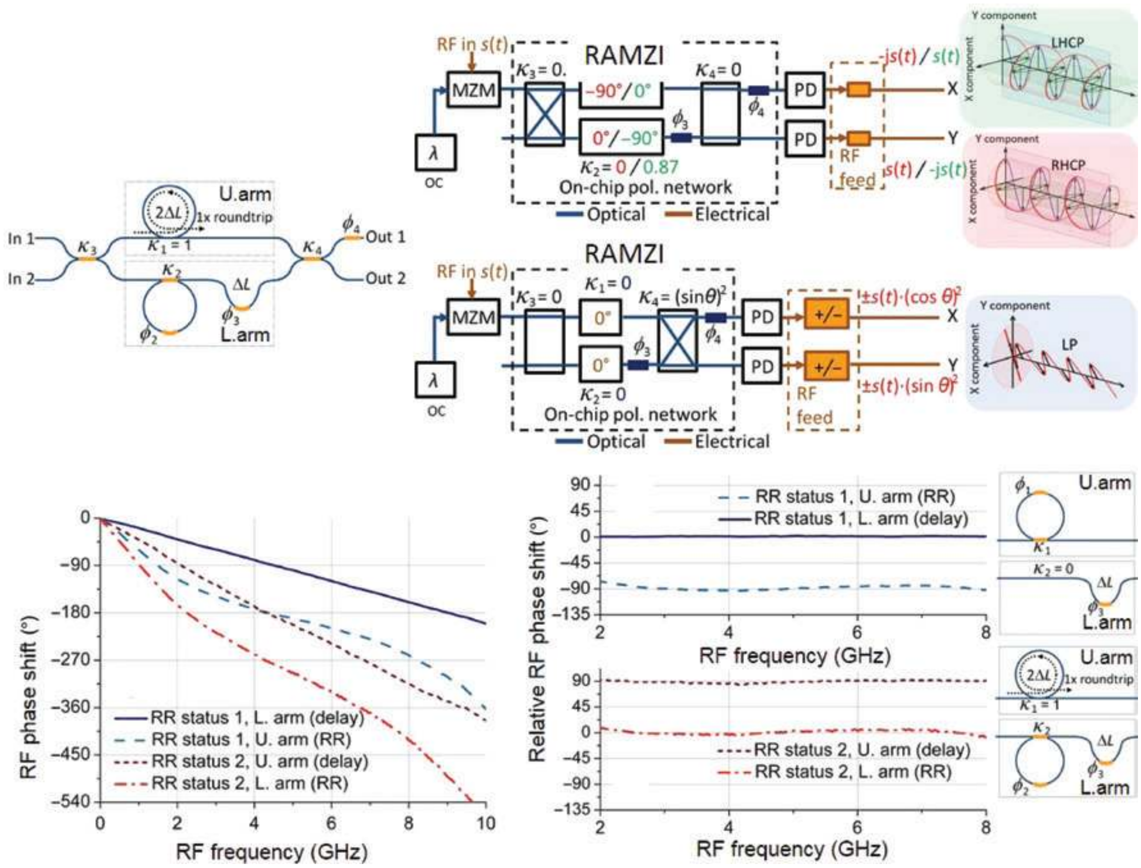

Figure 13: Design and realization of a highly reconfigurable RAMZI circuit: an application as a polarization network for dual-polarization linear antennas [79] (Copyright in 2013, Optical Society of America).

system performance and lower the system complexity. It should be mentioned that this work considered only one polarization of light due to the waveguide polarization sensitivity. A possible solution for this is to process two orthogonal polarizations separately using two such chips while having the polarization splitting and recombining performed off chip. However, this would incur issues on several matters, for example, inter-polarization phase locking, additional losses, and control complexity. A more desired solution is a low-loss waveguide that supports both polarizations and enables monolithic implementation of the processing functions. Silicon and indium phosphide platforms are possible candidates to use, but need further improvement on waveguide loss, particularly when delay path lengths of tens of centimeters are required on chip. Other investigations of TriPleX also demonstrated waveguide geometries with a box-like shape [10] which reduces the polarization sensitivity. However, the increased sidewall roughness incurs higher loss and therefore needs to be considered as a trade-off for different applications.

5.4 Desirable features

The design flexibility of such processor chips, thanks to the building block paradigm, enables a large variety of circuit architectures. We presented a processor chip comprising an RAMZI incorporated in a Sagnac loop [84] as shown in Figure 15. While the circuit variation is as simple as adding a connecting waveguide between two complementary ports of the RAMZI, this design equals a two-stage RAMZI nested in a lattice structure and enables a comb filter with a record small 3-dB passband bandwidth of 600 MHz for the optical filters of this kind [48]. Next to the possible applications for RF filters, Geng et al. utilized this sharp frequency selectivity to implement an optical pulse repetition rate multiplexer which increases the comb line interval of a periodic pulse train's frequency comb spectrum by means of filtering. This function is of high interest to be used together with integrated optical pulse train sources [85] that provide the desired high device compactness and stability but lack pulse rate changing capability. In [84], two experiments of five-time multiplications

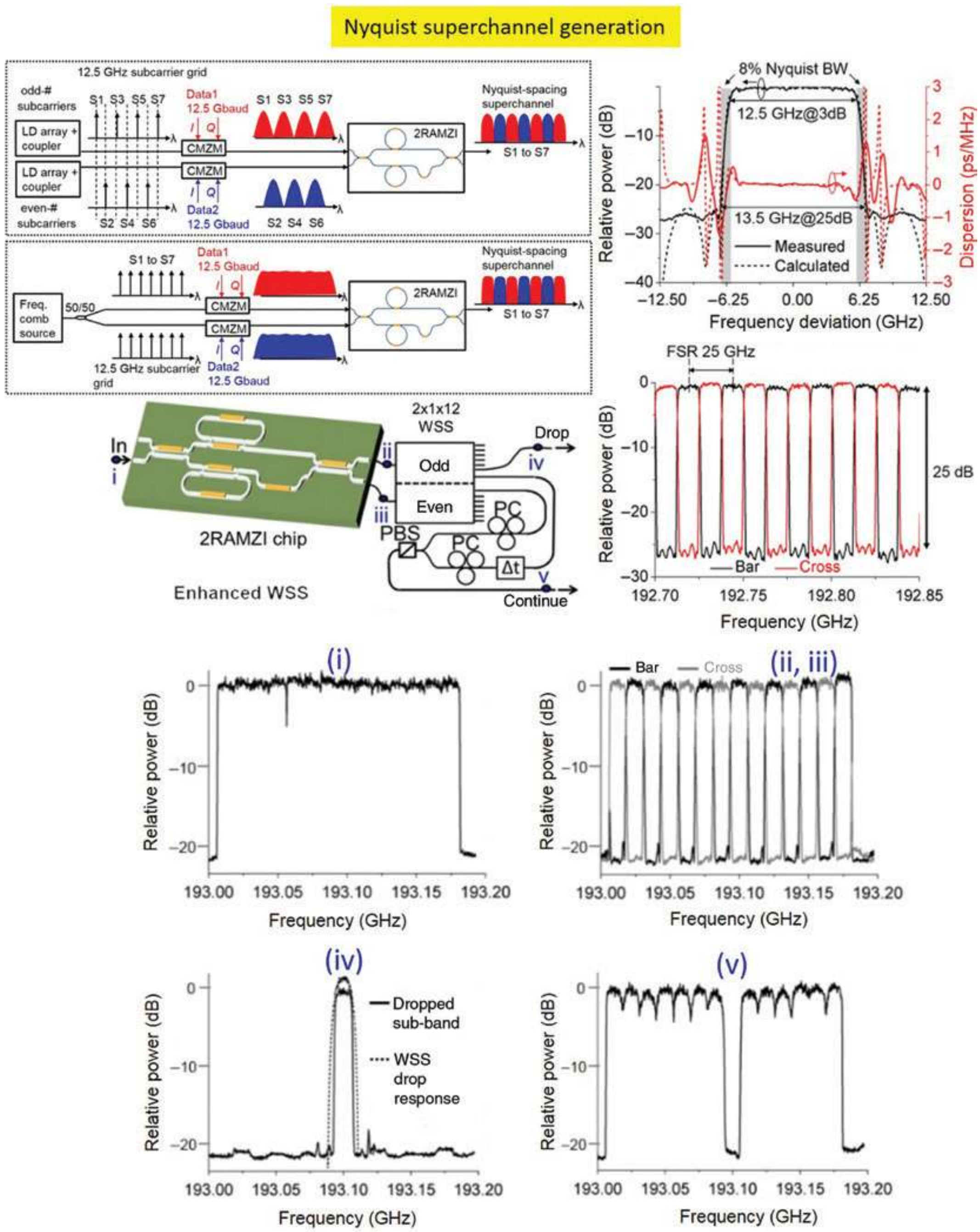

Figure 14: Design and realization of a highly reconfigurable RAMZI circuit: an application as a Nyquist-filtering interleaver for WDM super-channel multiplexing and demultiplexing [55] (Copyright in 2016, Optical Society of America).

were successfully demonstrated, that is, from 2.5 to 12.5 Gpulses/s and from 10 to 50 Gpulses/s. As another key result of this work, the measured filter shape exhibits high performance across the entire telecommunication C-band, covering a usable bandwidth wider than 4 THz, which proves an important capability of the waveguide technology that is highly desired by many applications in fiber communication systems and networks [11, 81].

6 Programmable optical chip

6.1 2D lattice mesh network topology

In the past few decades, integrated optical signal processors have undergone a rapid advancing with a significant increase in complexity and performance, not only driven

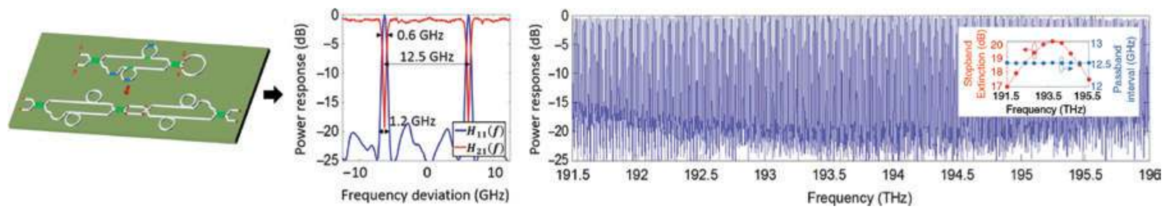

Figure 15: Design and realization of a highly reconfigurable RAMZI circuit: implementation of a full C-band comb filter with an RAMZI incorporated in a Sagnac loop [84].

by the applications in optical communication networks and microwave photonics, but also by many other emerging fields such as optical sensing, biophotonics, and quantum optics [16, 17, 86]. To date, a large number of such processors have been demonstrated, and the realization of most of them is based on the so-called application-specific photonic integrated circuits (ASPICs). In these, a particular circuit and chip configuration are designed to perform a specific function, for example, like the aforementioned processor chips for microwave photonic implementations of RF filters.

This trend, however, is leading to a considerable amount of fragmentation in the field, that is, where the number of technological solutions is almost equal to the number of applications. As a result, the market for many of these application-specific technologies is too small to justify their further development into cost-effective industrial-volume manufacturing processes.

A radically different approach in contrast to ASPICs is so-called programmable optical chips [87], that is, universal signal processors integrated on optical chips. By programming such a processor suitably, it is possible to implement different functions as desired. This is a similar concept as digital signal processors and FPGAs in microelectronics, where, through a software-defined approach, common hardware is shared for multiple functionalities.

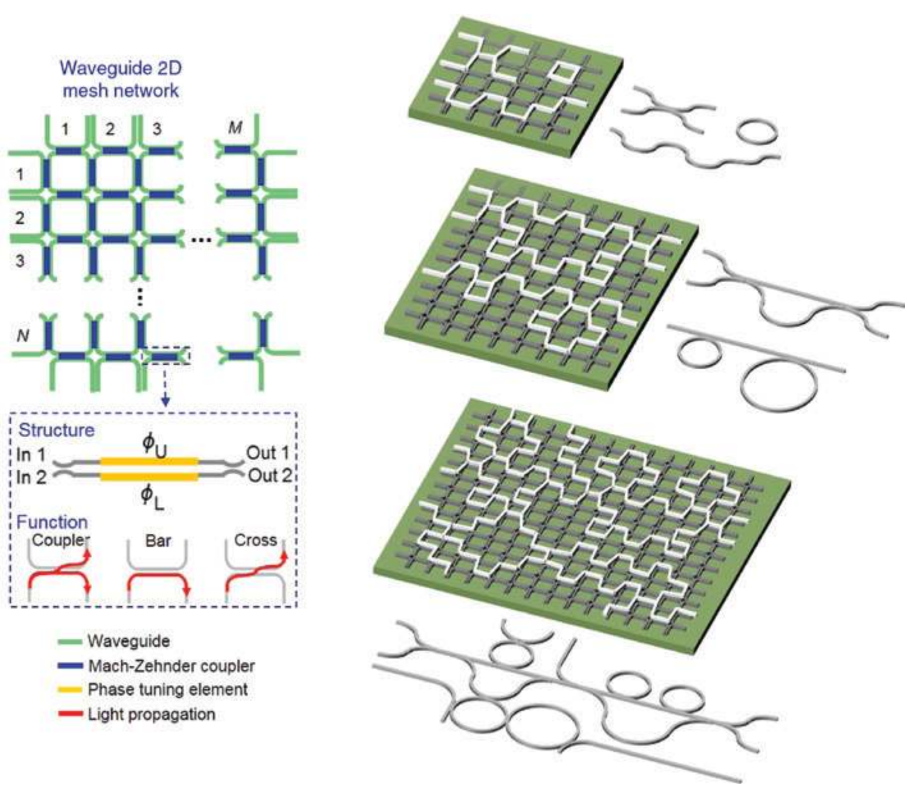

Figure 16: Conceptual design of a programmable optical chip comprising a number of Mach-Zehnder couplers interconnected in a 2D lattice mesh network architecture and examples of implementing different signal processing circuit topologies [45] (Copyright in 2015, Optical Society of America).

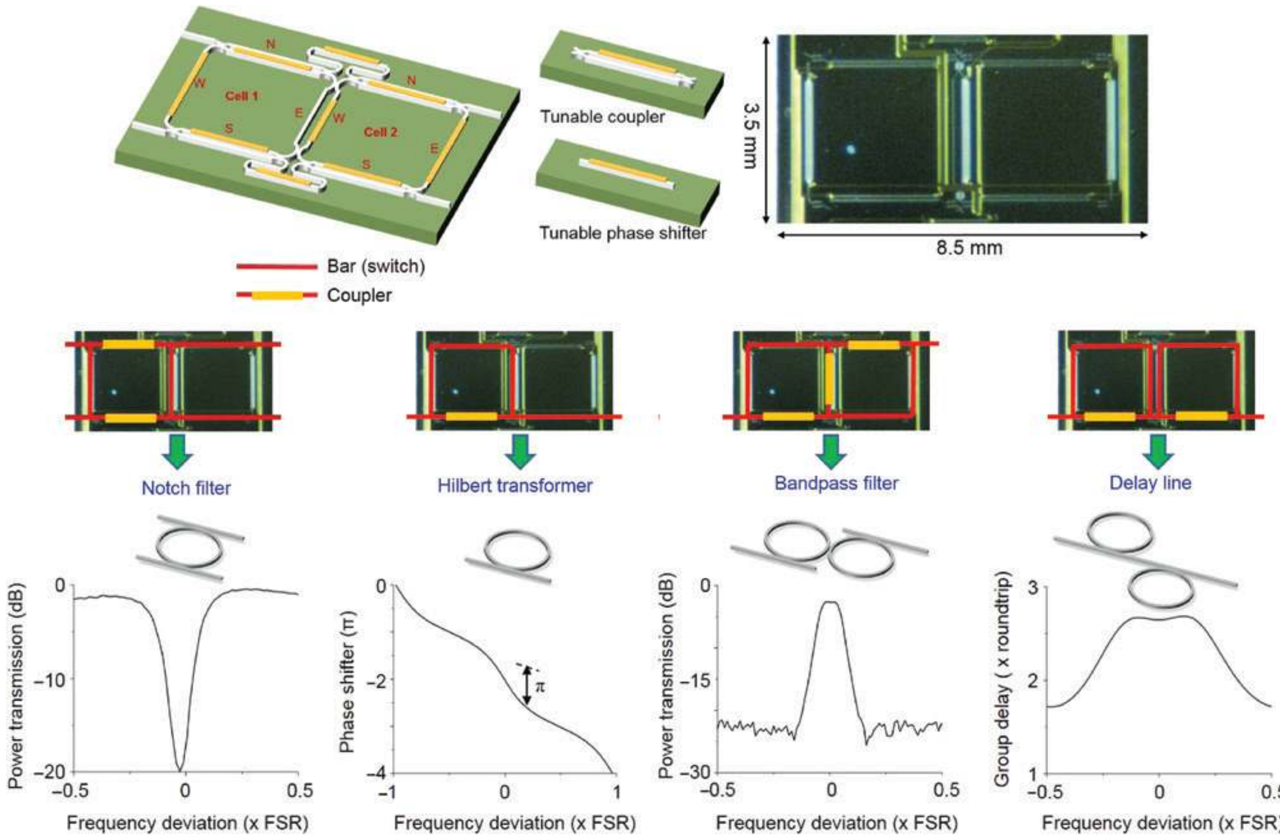

Figure 17: A proof-of-concept device fabricated in TriPleX technology, which comprises two mesh cells, and demonstration of its programmability [45] (Copyright in 2015, Optical Society of America).

For the implementations of RF filters, this on-chip programmability translates the optical reconfigurability and function variety into the RF domain, and therefore plays a key role for realizing near-DSP flexibility in microwave photonic implementations of RF filters. Inspired by this concept, we proposed a first design of a programmable optical signal processor chip [45] and experimentally demonstrated, as an application example, its use for the implementation of a highly reconfigurable RF filter. The chip comprises a number of identical Mach-Zehnder couplers that are interconnected in the topology of a two-dimensional lattice mesh network as shown in Figure 16. The Mach-Zehnder couplers have their both arms equipped with phase tuning elements. This design allows each Mach-Zehnder coupler to be configured to perform either a 2×2 coupler or an optical path routing switch, with the capability of simultaneously controlling the optical phase, and therewith serving as a basic programmable unit. In principle, when provided with a sufficiently large network scale, one can program those Mach-Zehnder couplers to implement an arbitrary interferometric circuit topology for signal processing purposes, for example, FIR and IIR filters, with full control of circuit parameters (amplitude and phase of each optical path in the circuit). Alternatively, one can also implement a multi-port switch network or a bank of parallel signal processing functions, the freedom of which is enabled by the programmability introduced on the optical chip.

Figure 17 shows a proof-of-concept device comprising two mesh cells, fabricated in TriPleX technology. In the experimental demonstration, four out of more possible examples of distinctly different circuit topologies were implemented using the same chip and their functions were verified by spectral measurements.

6.2 Various lattice mesh network designs

In a following study of the lattice mesh network design, Pérez et al. [88] made an extensive comparison between three different lattice mesh geometries, that is, triangular, square, and hexagonal lattice meshes. The square lattice mesh offers highest routing flexibility of the optical paths for a certain circuit function, or in other words, the square mesh allows the most possible circuit topologies to be implemented in the lattice mesh network for a certain circuit function. The hexagonal lattice mesh is the most suitable option for implementation in terms of circuit complexity and fabrication challenges. Regarding the design of the Mach-Zehnder coupler as the basic building block, it is desired to have features with a small size to allow for finer optical path length resolution, low loss and low power consumption for the tuning elements. Of further importance is the capability of a full tuning range of the power coupling ratio, that is, from 0 to 1, to guarantee the provision of programmability. A variety of designs have been demonstrated to date in these regards. Recently, for example, Wang et al. [89] demonstrated an RF arbitrary waveform generator using a silicon circuit with tunable couplers in the order of tens of micrometers; Dai et al. [90] demonstrated such couplers with a bandwidth of 140 nm and an excess loss <1 dB; Suzuki et al. [91] and Miller [92] showed designs based on lattice cascades of multiple Mach-Zehnder couplers with higher fabrication tolerances. The consideration of all this could be of use for the further development of programmable optical chips which, as one important application, serve as the engine for microwave photonic implementations of reconfigurable RF filters. Furthermore, as identified to be a key technology, programmable optical chips are receiving a great amount of research and development effort at present [87, 93]. Demonstrations of software-defined signal processing functions on fully integrated processor devices that combines both electronics and optics are expected to be made in the near future [94].

7 Device and system development

7.1 Photonic integrated circuit technologies

PIC technologies have experienced a rapid advance in the past few decades. At present, the ever-growing progress of large-scale integration already allows for thousands of components to be fabricated on one chip [15, 21]. This capability sets the stage for the chip-scale realization of complex optical systems which enables a range of technologies for modern devices and instrumentation that utilize optical properties. While many materials are still in their infantry or need a great amount of improvement before reaching industrial maturity, a number of materials, such as SOI, Si_3N_4, and InP, have demonstrated a wide range of circuit functions with high performance and therewith promise the establishment of an industrial optical hardware platform. In assistance to this goal, the business model of the multi-project-wafer run and generic foundry provides an effective path to boost the development of PIC technologies, where not only the powerful companies but also the cost-sensitive units such as university research groups and emerging small-size companies are able to afford the access to the state-of-the-art fabrication facilities and thereby play the role of PIC developers.

Currently, extensive investigations are being conducted on various materials, each having pros and cons. In general, SOI allows for the highest device compactness and has the potential of hybrid electrical-optical monolithic integration, featuring high compatibility with CMOS processes and potential for low-cost fabrication. Many foundries, such as IMEC, AIM Photonics, and Global Foundries, offer relatively mature silicon platforms to further promote its development. A great challenge here is the integration with light sources due to the difficulty of lasing directly in silicon. However, recent advances in hybrid integration of InP and silicon have shown remarkable results tackling this issue [32]. The InP platform features the capability of providing a full range of high-performance active functions including lasers, amplifiers, modulators, and photodetectors [20]. This uniqueness forms the foundation of monolithic

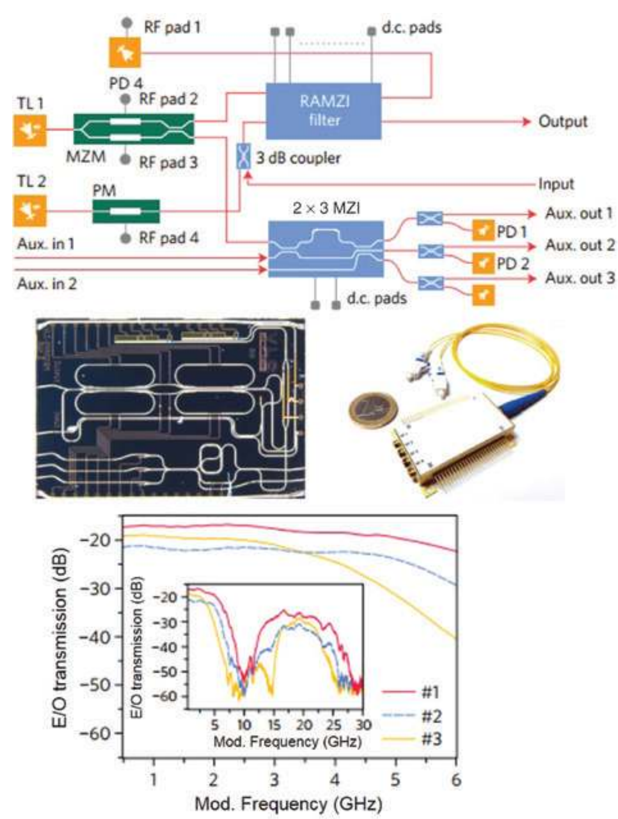

Figure 18: A monolithic integrated photonic microwave filter in InP [28] (Copyright in 2017, Nature Photonics).

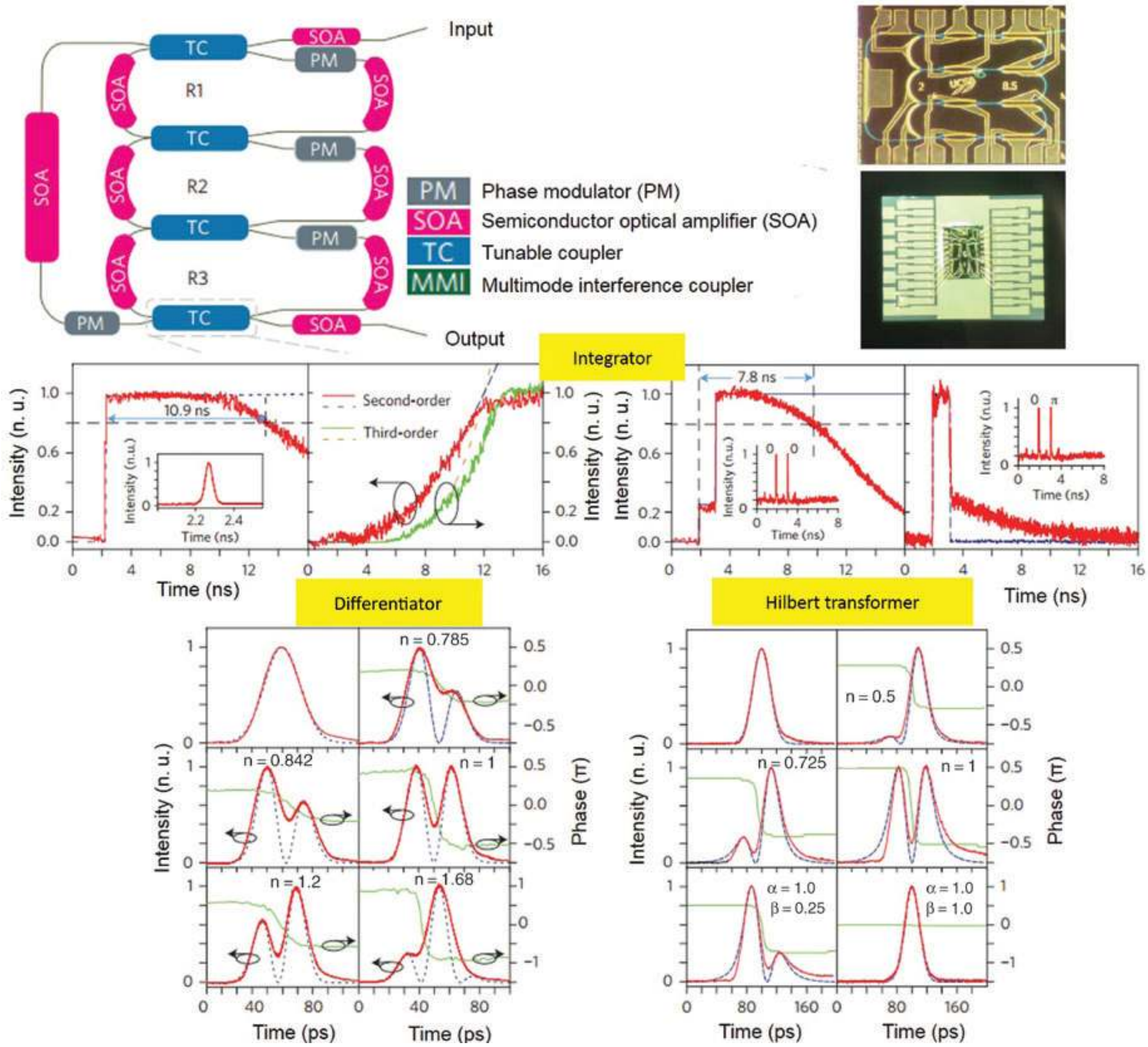

Figure 19: A reconfigurable photonic signal processor in InP [96] (Copyright in 2016, Nature Photonics).

integration of complete optical systems, together with practical features of small bend radii and low polarization sensitivity. As InP platforms provide both active and passive functions, which support most PIC applications, a potential advantage of low packaging costs may play a key role for their proliferation, particularly for large-scale integration scenarios. An increasing number of foundry services such as Oclaro, Fraunhofer Heinrich Hertz Institut (HHI), and COBRA spinoff company SMART Photonics are endeavoring to improve this technology. However, further efforts are still needed for the issues such as waveguide propagation loss and dispersion. Passive platforms such as Si_3N_4, SiO_2, and SiOH demonstrate good performance in terms of propagation loss [16]. However, for complex functions such as an integrated photonic beamformer, their integration with active functions requires micro-assembly of multiple chips with each providing a different function. In this case, a great challenge is the finding of particular packaging solutions. Moreover, some nonlinear materials such as periodically poled lithium niobate (PPLN) and chalcogenide (As_2S_3) are also gaining interest because of their unique nonlinear properties in optical signal processing [10, 95]. However, the possibility of their integration with functions in other materials for creating integrated complex optical signal processors still requires further investigations.

In a broader sense, realizing chip-scale integration of the entire designed function is a key step for reaching the goal of ultimate device stability and low fabrication cost. These are the two most important factors for the proliferation of microwave photonic solutions in RF engineering for practical applications. In the past few decades, a great amount of effort has been made for this purpose, leading to significant advances in fabrication

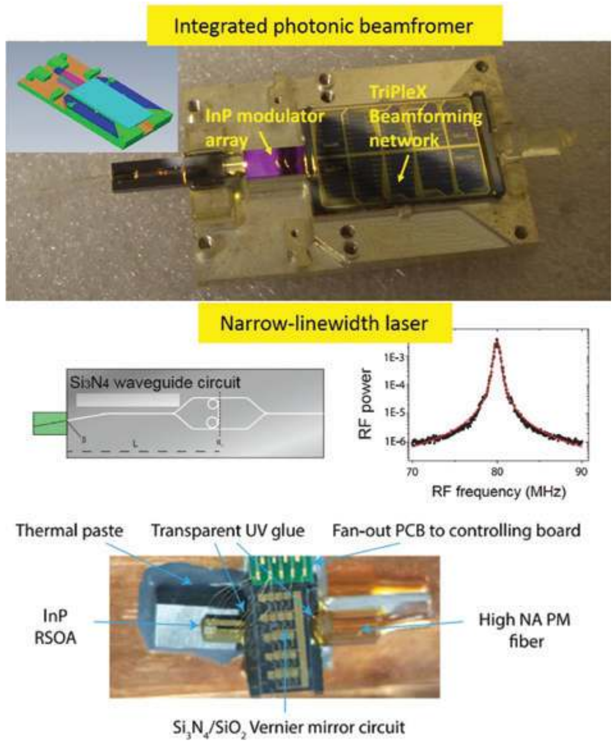

Figure 20: An integrated photonic beamformer and a narrow-linewidth laser based on a micro-assembly with InP-TriPleX hybrid integration [32, 97] (Copyright in 2015, Optical Society of America, Copyright in 2014, IEEE).

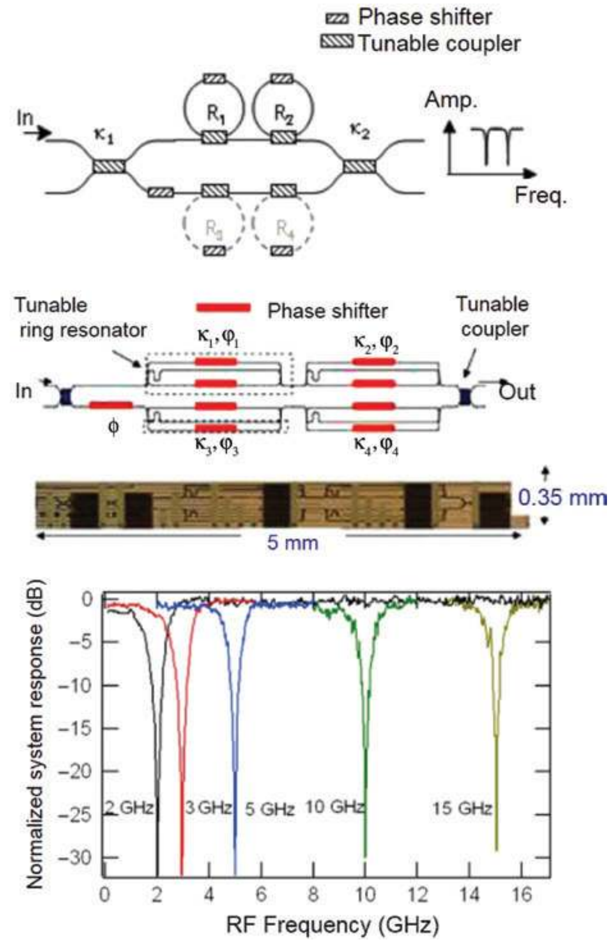

Figure 21: An RF notch filter implemented using an RAMZI circuit in silicon [98] (Copyright in 2007, IEEE).

technology, materials, functional designs, and application development. In a recent work, Fandiño et al. [28] demonstrated a monolithic integrated photonic microwave filter fabricated in an InP waveguide platform where for the first time the whole designed function including both active and passive components reached a 100% level of integration on a single chip as shown in Figure 18. This work not only shows the current maturity of the photonic integration and packaging technology, but also demonstrates the potential capabilities of the generic foundry fabrication model that is expected to provide an effective path for the fast development of PIC-based applications. In the direction toward fully programmable integrated signal processors, Liu et al. [96] have demonstrated a photonic integrated circuit fabricated in a similar waveguide platform that is able to be electrically reconfigured to implement multiple, different signal processing functions as shown in Figure 19. The circuit architecture studied in that work is anticipated to inspire more complex designs of such processors and a wide variety of signal processing functions. Alongside the monolithic integration approach, hybrid integration by means of a micro-assembly of multiple chips fabricated in different waveguide technologies has also made remarkable progress in the recent years. In particular, such hybrid integration of active components in InP and passive components in TriPleX combines the best of both worlds, leading to optimization of device performance. One example of such hybrid integration is an integrated photonic beamformer using a modulator array in InP and a true-time-delay beamforming network in TriPleX [97] as shown in Figure 20. Also shown in Figure 20, Fan et al. [32] recently demonstrated a narrow-linewidth laser which is based on a micro-assembly of a gain medium in InP and an external highly selective, low-loss filter in TriPleX. In this work, a key packaging challenge of chip-to-chip coupling loss is addressed, which is critical for the performance of the laser.

7.2 Various filter implementations

In the past decade, a number of groups have made significant contributions to the study of integrated optical signal processors, using different waveguide technologies and circuit designs, and many of them have explored their applications for microwave photonics including RF filters. Next to Si_3N_4, other waveguide platforms such as silicon, III–V materials, polymer, and chalcogenide glass have demonstrated many capabilities and features for optical signal processing. A number of representative works showed clear possibilities of creating programmable integrated optical signal processors and demonstrated their promising use in RF engineering.

Using silicon waveguides, Rasras et al. [98] demonstrated processor chips comprising a particular RAMZI circuit as shown in Figure 21 and their use for implementing bandpass and notch types of RF filters. The processor chips feature a waveguide propagation loss of 0.25 dB/cm and a filter bandwidth smaller than 1 GHz for an FSR of 13.5 GHz. In Dong et al. [99], demonstrated silicon processor chips comprising coupled RRs up to fifth order as shown in Figure 22, which feature a propagation loss of 0.5 dB/m and provide bandpass filters with GHz-level bandwidths. Also in silicon waveguides, Orlandi et al. [100] demonstrated a processor design of an unbalanced MZI loaded with a pair of RRs on the shorter arm as shown in Figure 23. This design enabled a waveguide filter with a wide bandwidth tunability, that is, from 10% to 90% FSR. As a strong example for a reconfigurable waveguide filter, Ibrahim et al. [101] demonstrated a design of a lattice

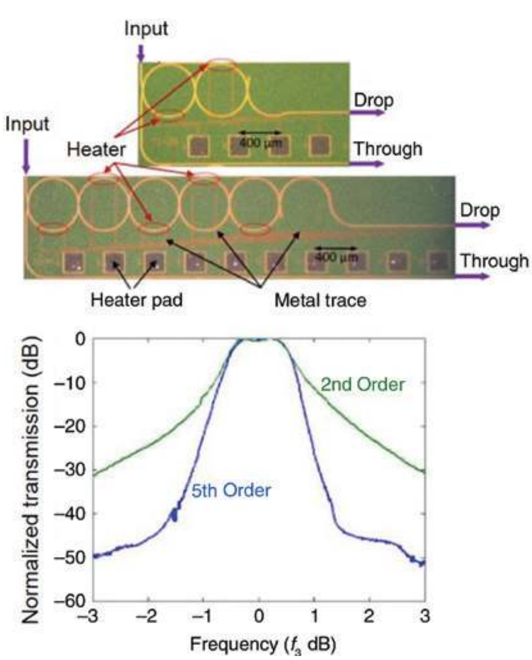

Figure 22: A tunable bandpass filter using a fifth-order coupled ring resonator in silicon [99] (Copyright in 2010, Optical Society of America).

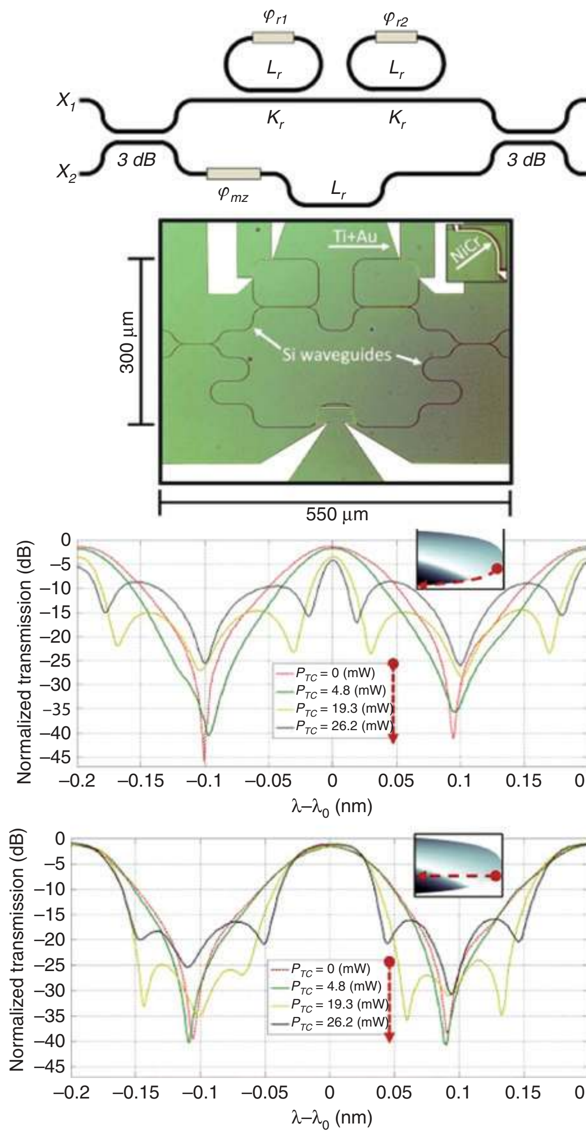

Figure 23: A bandwidth tunable filter in silicon [100] (Copyright in 2014, IEEE).

filter based on silicon unit cells arrayed in large-scale PICs as shown in Figure 24A. Each unit cell employs a combination of an RR and a MZI with tunable phase elements in both of the paths to enable separate control of the circuit parameters. This design combines two types of silicon rib waveguides, that is, a narrow type with a width of 0.5 µm for optimizing the tuning efficiency as well as enabling small bends and a wide type with a width of 3 µm for lowering propagation loss which measured to be 0.5 dB/cm. In Guan et al. [102], demonstrated the use of such a fourth-order reconfigurable lattice filter for microwave photonics.

For III–V materials, Norberg et al. [103] demonstrated a lattice filter integrated in an InP-InGaAsP waveguide, which is composed of two forward paths and contains one ring as shown in Figure 24B. The filter response can be configured by means of biasing the semiconductor optical amplifiers (SOAs) and phase modulators placed in the arms of the unit cells, whose frequency tuning range, for this particular design, measured to be about 100 GHz. Guzzon et al. [104] demonstrated an implementation of a tunable filter featuring zero insertion loss. This demonstration uses a coupled RR circuit with integrated SOAs as shown in Figure 24C. Utilizing the hybrid integration technology, Chen et al. [105] reported a microwave photonic filter using a processor chip that combines III–V quantum well layers bonded with low loss passive silicon waveguides as shown in Figure 25A, where the III–V quantum devices provide active tuning capability while low loss silicon waveguides are used for delay paths. III–V materials serve for optical signal processors with a much wider range of devices than interferometric filters and tuning elements. As an example of such devices, Sancho et al. [106] reported a 1.5-mm-long

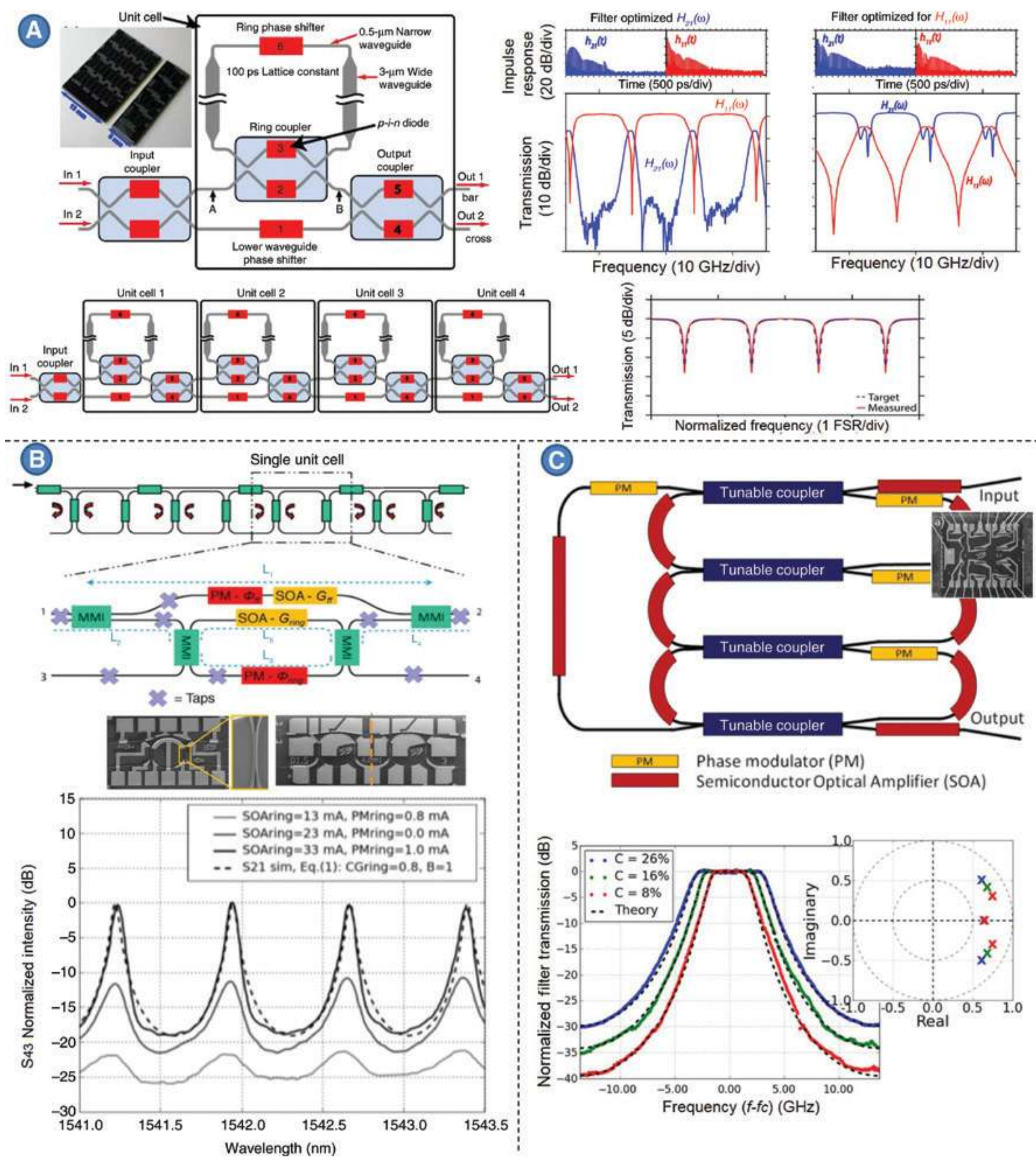

Figure 24: (A) A design of lattice filter in silicon (Figure 12) [102] (Copyright in 2014, IEEE). (B) A design of lattice filter in InGasAsP-InP [103] (Copyright in 2010, IEEE). (C) A design of a bandpass filter with zero insertion loss [104] (Copyright in 2011, Optical Society of America, IEEE).

photonic crystal waveguide capable of generating a controllable delay up to 170 ps with moderate losses. This device was demonstrated to be able to implement both notch and bandpass types of RF filters with a spectral tuning range of 50 GHz as shown in Figure 25B. There have also been extensive investigations of alternative nonlinear materials fabricated on chips for optical signal processing [107]. The initial studies are focused on the functions for fiber transmission systems and communication networks, such as wavelength conversion, optical time lens, and optical sampling. More recently, RF functions enabled by such devices are explored including a number of remarkable demonstrations of RF filters. Ziyadi et al. [108] demonstrated an RF filter with variable bandwidth, shape, and center frequency using an optical tapped delay line based on an optical frequency comb and a PPLN waveguide as shown in Figure 26A. Here, the tap coefficient generation and multiplexing are enabled simultaneously by the PPLN waveguide's sum frequency generation (SFG) and difference frequency generation (DFG) effects [95]. On-chip stimulated Brillouin scattering (SBS) is another nonlinear effect that has been explored for implementing RF filters. Utilizing the SBS effect in a 6.5-cm-long As2S3 waveguide, Morrison et al. [109], Byrnes et al. [110], and Choudhary et al. [111] demonstrated respectively an RF bandstop filter and narrow bandpass filter with tunable bandwidth and center frequency as shown in Figure 26B. In a later work Marpaung et al. [44], associated such SBS effect with a particular modulation spectrum comprising uneven sidebands and therewith demonstrated a highly selective RF notch filter with a very deep notch of 60 dB and a large frequency tuning range of 30 GHz as shown in Figure 27A. Recently, aimed to facilitate the integration of the SBS effect with other processing functions on a chip, Casas-Bedoya et al. [112]

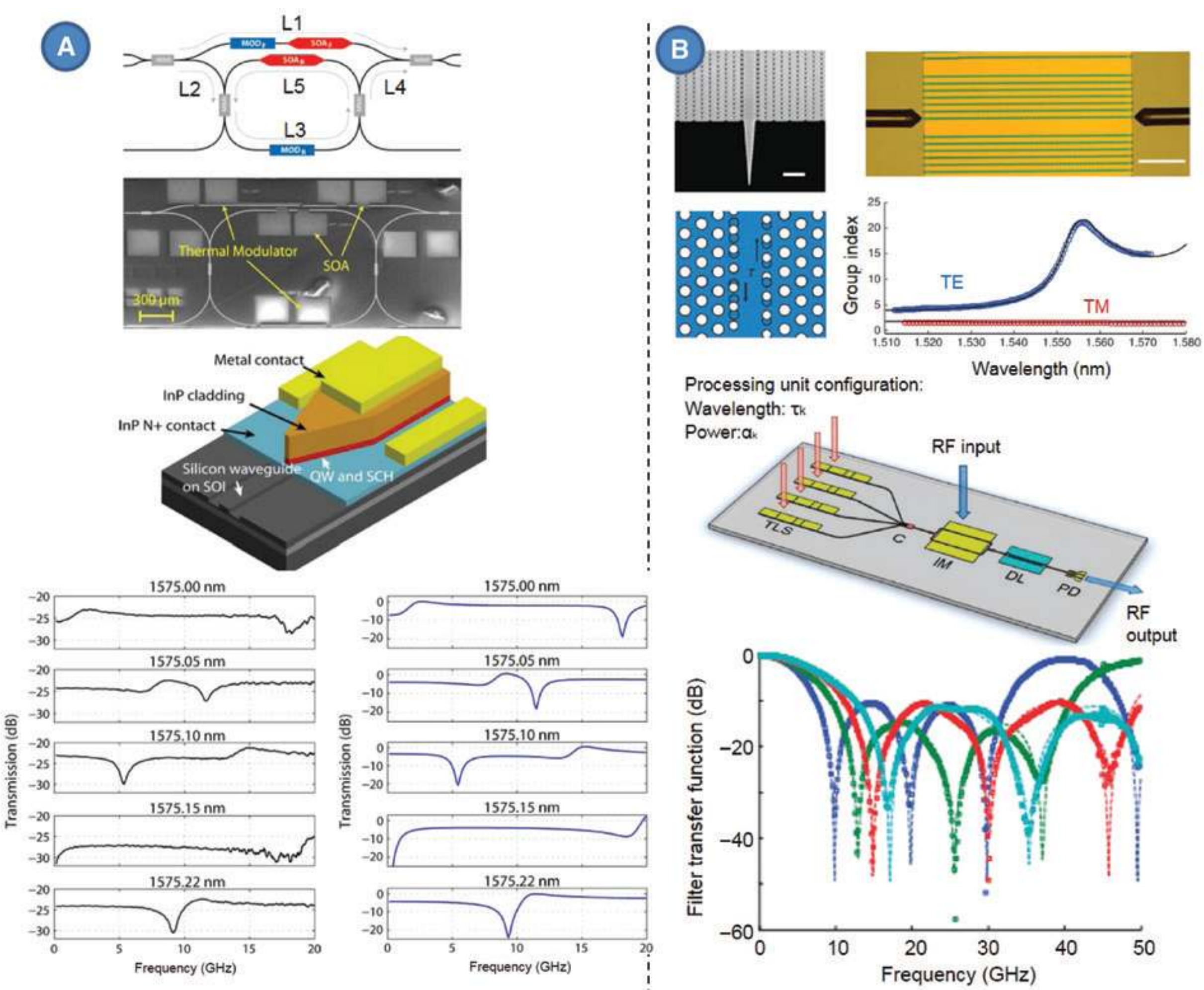

Figure 25: (A) An RF filter implemented using an InP-silicon hybrid circuit [105] (Copyright in 2010, IEEE). (B) An implementation of an RF filter using a photonic crystal waveguide in InP [106] (Copyright in 2012, Nature Communications).

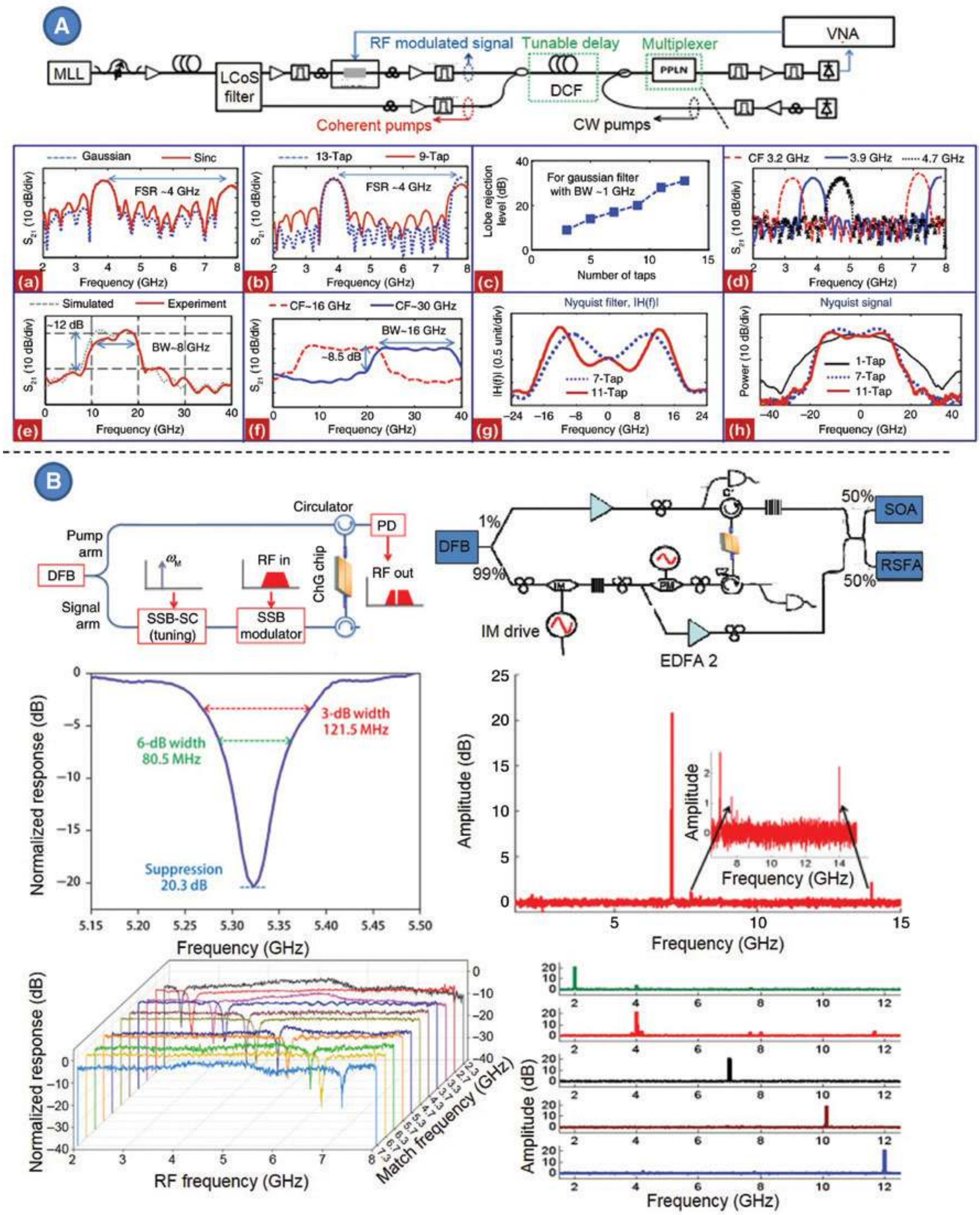

Figure 26: (A) An RF filter implemented using a PPLN waveguide [108] (Copyright in 2015, Optical Society of America). (B) Implementations of bandstop and bandpass RF filters based on SBS in an As_2S_3 waveguide [109] (Copyright in 2014, Optics Communications).

demonstrated a similar RF filter function using a silicon waveguide that has its substrate particularly treated to provide high SBS efficiency as shown in Figure 27B.

All these on-chip processing functions, linear or nonlinear, have made important contributions for photonic solutions in RF engineering. The associated waveguide technology development paves the way for creating programmable integrated optical signal processors. To give a snapshot of progress, Table 1 lists a number of representative works on microwave photonic

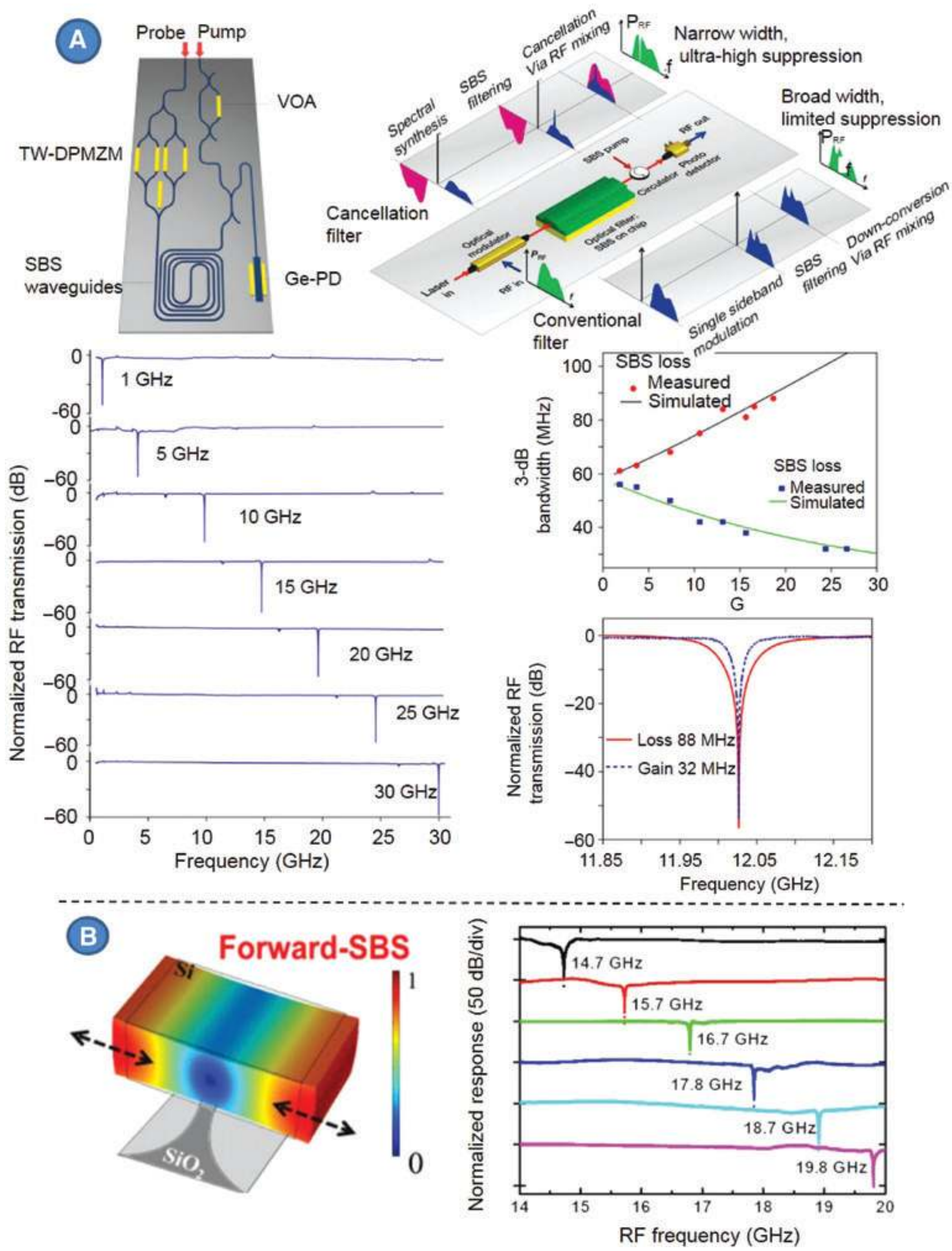

Figure 27: (A) A highly selective RF notch filter implemented using a combination of SBS in an As_2S_3 waveguide and modulation spectrum shaping [44] (Copyright in 2015, Optical Society of America). (B) An RF notch filter implemented based on SBS in a silicon waveguide [112] (Copyright in 2015, Optical Society of America).

implementations of RF filters using optical signal processor chips [113–116].

7.3 Control subsystems

Regarding the control, the complexity increases exponentially with the number of tuning elements on each chip. Conventional approaches to configure the circuits need pre-characterization of each tuning element and inter-element crosstalk in the circuit and use an open-loop control based on look-up tables [102, 117]. These methods are common to use for simple chip designs. However, for complex circuits that comprise a large number of tuning elements, a dedicated control algorithm needs to be devised, which in practice can be applied by means of real-time computing or switching between different tuning element statuses [118]. Generally, the control can

Table 1: Some recent representative works of integrated microwave photonics RF filters using optical signal processor chips.

References	Filter type	Material	Structure	Bandwidth 3-dB (GHz)	Center freq. (GHz)	Max. power ext.	Tuning elements	Bend radius (μm)	Tunning mech.	Tuning efficiency (mW/π)
[52]	A	Silicon	RR, MZI	0.635	2–15	33	9	7	TO	9
[60]	B	Silicon	RR	18	10–85	10	N.A.	20	OP	Off-chip
[113]	B	Silicon	RR, MZI	1.25	0–20	20	9	25	TO	15
[103]	B	InP-InGaAsP	RR	1.9–5.4	0–27	32	31	150	EO	Off-chip
[56]	A	TriPleX	RR, MZI	0.5	0–1	30	11	125	TO	0.25
[114]	B	Silicon	RR, MZI	0.9–5	0–12	38	16	20	TO	20-30
[110]	B	As_2S_3	Waveguide	0.023	2–12	20	N.A.	N.A.	OP	Off-chip
[106]	B	InP PhC	Waveguide	8–30	0–50	50	N.A.	N.A.	EO	Off-chip
[61]	A	TriPleX	RR	0.247–0.84	2–8	66	1	125	TO	0.25
[109]	A	As_2S_3	Waveguide	0.126	2–8	20	N.A.	N.A.	OP	Off-chip
[115]	A	Silicon	RR	6–9.5	2.5–17.5	40	N.A.	75	OP	Off-chip
[74]	B	TriPleX	Waveguide	0.072	0–1	51	17	125	TO	0.25
[116]	A	Silicon	RR	0.06	12.4–30.6	60	N.A.	10	OP	Off-chip
[45]	A/B	TriPleX	2D lattice mesh network	1.5/0.8–1.6	1.6–6	25	9	125	TO	0.25
[112]	A	Silicon	Waveguide	0.098	14–20	48	N.A.	N.A.	OP	Off-chip
[44]	A	As_2S_3	Waveguide	0.06–0.09	0–30	56	7	N.A.	OP	Off-chip
[108]	B	PPLN	Waveguide	1–3	3–7	20	N.A.	N.A.	OP	Off-chip
[111]	A	As_2S_3	Waveguide	0.03–0.44	0–30	24	N.A.	N.A.	OP	Off-chip
[63]	A/B	TriPleX	RR	2.7/1.2–2.5	2.75–10.25	40	6	125	TO	0.25
[28]	B	InP-InGaAsP	RR, MZI	10	0–4	35	6	150	EO	N.A.
[51]	A	Hybrid silicon	RR	0.8	0–20	6	4	N.A.	EO	Off-chip

A, Notch filter; B, bandpass filter; EO, electro-optical; MZI, Mach-Zehnder interferometer; OP, optical pump/laser; RR, ring resonator; TO, thermo-optical.

be divided into two tasks: one is locking or stabilizing the circuit in a well-defined status free of drifts; the other is to reconfigure the circuit to different functions as desired.

The proper operation of these requires a fast feedback mechanism. Typically, the feedback signals are extracted by means of monitoring optical powers, which in practice can be performed by tapping off a defined portion of the light from targeted optical paths [119] or using contactless integrated photonic probes (CLIPPs) [120]. Several representative examples have been demonstrated. In [121], automatic reconfiguration and optical routing of a silicon photonic switch fabric based on Mach-Zehnder interferometers (MZIs) are illustrated, where CLIPPs provide real-time information on the routing path, allowing an easy sequential tuning and feedback controlled stabilization of the individual switching elements. In [122, 123], a work on spatial reconfigurable add-drop multiplexers is presented, having the splitters and combiners controlled via a simple algorithm implementable using a local electronic feedback loop. In [124], a dedicated control subsystem comprising programmable electrical logic devices and drivers is presented, which performs automated path scheduling and assessment of a complex wavelength-and-space-switch circuit. In these examples, electrical devices such as computers, power sources and amplifiers, and/or digital microprocessors or FPGAs are used. Several issues should be addressed in the future development of control subsystems, including electrical-optical interface, power consumption, and system integration.

It should also be mentioned that in some cases the device operation stability, for example, control of thermal drifting, can be implemented inherently by means of material engineering. For example, polymers materials [125–127] with negative thermo-optic coefficient can be added to silicon waveguides to provide effective reduction of their thermal sensitivity.

8 Conclusions

This paper gives a review of the recent progress in integrated microwave photonics programmable chips and their applications of RF filters. The discussions focus on the design and applications of integrated optical signal processors in TriPleX waveguide technology that have been demonstrated in the past decade and also refer to a number of representative works using other material platforms that have made great contributions and raised inspirations in this area.

The issues of bandwidth limitation and power consumption of the RF electronics and the intrinsic advantages of photonics in these aspects as well as the promising applications of analog photonic links for RF communication systems and access networks provide clear motivations for the search of photonic solutions for RF front ends. This will either bring new features to the existing functions or enable new functions that set the stage for the next-generation system improvement and innovation. The great use and commercial success of electronic programmable signal processors such as FPGAs provide a convincing rationale for the pursuit of their optical counterparts. If the concept of creating a programmable optical signal processor chips using a two-dimensional lattice mesh network of Mach-Zehnder couplers can be further developed and scaled, its impact in photonic-based RF processing will be unquestionable. For one thing, microwave photonic system costs will be greatly reduced as they will benefit from the economies of scale of integrated fabrication, especially if the mesh architecture can be implemented using current state-of-the-art generic integration and generic foundry models. Besides, microwave photonic systems oriented to the generation and processing of microwave and millimeter-wave signals will benefit from the compactness of integrated optics technologies. Programmable optical signal processors have strong potential use for RF engineering such as Internet of Things, medical imaging systems using terahertz waves, sensor interconnection in wireless broadband personal area networks, wearable communication devices, and miniature base stations for femtocell fiber-wireless multiservice radio access networks. Beyond these, they promise interesting applications in many other areas too, such as realizing a multifunctional lab on a chip in biophotonics, reconfigurable logic gates in quantum information systems, software-defined reconfigurable filters, and switching as well as routing fabrics in optical communication networks.

However, further development of this concept toward commercial use still faces a number of significant questions and challenges. One key question refers to the choice of material platforms for realizing such a chip. None of the current technologies seem to cover the full range of requirements. Indium phosphide is the only technology capable of providing active elements such as lasers and amplifiers. It is certainly the most complete in terms of available components but is quite lossy. Silicon brings compatibility with CMOS fabrication processes and low-loss passive components, but it is not suitable for implementing optical sources and amplifiers. Silicon nitride provides passive components with extremely low losses, MHz-band frequency resolution, and working wavelength range covering the full telecom C-band. However, it is not suitable for implementing active devices despite its potential for modulators [128]. While the monolithic approach requires less effort in packaging, hybrid approach, particularly the recently demonstrated InP-TriPleX assemblies, shows a bright prospect for chip-scale realization of complex optical systems comprising both active and passive components.

Regarding the chip design, a challenge is to implement a mesh network with a sufficient number of cells within a feasible space on the chip. The proof-of-concept demonstration mentioned above uses a 2×1 cell scheme in TriPleX where each cell requires an area of 3.5×3.5 mm^2. To realize a mesh network on a larger scale, it may be necessary to turn to material platforms that provide a higher refractive index contrast and thus smaller waveguides, such as SOI. Yet, even in this case, a complex mesh will require strict control of waveguide uniformity and roughness along the whole structure to guarantee homogeneous performance. A recent collaboration between ITEAM Research Institute of Polytechnic University of Valencia and Optoelectronics Research Centre of University of Southampton has led to a promising result of a SOI mesh network with seven hexagonal cells [129, 130].

Another challenge relates to power consumption and heat dissipation. The use of thermo-optical tuning elements mandates careful control of chip temperature and optimized designs of waveguide and heaters, which may increase the device size. Solutions to this limitation may be achieved by resorting to material platforms featuring electro-optical tuning.

The possibility of developing a programmable optical chip as a general-purpose signal processor is becoming a popular area of research, not only because of the potential for low fabrication costs, but also because it points to the tantalizing prospect of software-defined functions and systems on a miniaturized optical chip. This means an important transition in integrated optics that changes the paradigm from single devices and very simple circuits to complex systems featuring easy operation and high flexibility, like the transition that led to a great boost in electronics.

Acknowledgments: This work is funded by Australian Research Council under grants FL130100041 and CE110001018.

References

[1] Andrews JG, Buzzi S, Choi W, et al. What will 5G be? J Sel Areas Commun 2014;32:1065–82.
[2] Ridgway RW, Dohrman CL, Conway JA. Microwave photonics programs at DARPA. J Lightwave Technol 2014;32:3428–39.
[3] Capmany J, Muñoz P. Integrated microwave photonics for radio access networks. J Lightwave Technol 2014;32:2849–61.
[4] Capmany J, Novak D. Microwave photonics combines two worlds. Nat Photon 2007;1:319–30.
[5] Yao J. Microwave photonics. J Lightwave Technol 2009;27: 314–35.
[6] Seeds AJ, Williams KJ. Microwave photonics. J Lightwave Technol 2006;24:4628–41.
[7] Iezekiel S. Microwave photonics: devices and applications, 1st ed. UK, Wiltshire, Wiley, 2009.
[8] Rappaport TS, Murdock JN, Gutierrez F. State of the art in 60-GHz integrated circuits and systems for wireless communications. Proc IEEE 2011;99:1390–436.
[9] Marpaung D, Roeloffzen C, Heideman R, Leinse A, Sales S, Capmany J. Integrated microwave photonics. Laser Photon Rev 2013;7:506–38.
[10] Roeloffzen CGH, Zhuang L, Taddei C, et al. Silicon nitride microwave photonic circuits. Opt Express 2013;21:22937–61.
[11] Pant R, Marpaung D, Kabakova IV, Morrison B, Poulton CG, Eggleton BJ. On-chip stimulated Brillouin scattering for microwave signal processing and generation. Laser Photon Rev 2014;8:653–66.
[12] Cox CH. Analog optical links: theory and practice, 1st ed. Cambridge, Cambridge University Press, 2004.
[13] Doerr C. Silicon photonic integration in telecommunications. Front Phys 2015;3:7.
[14] Komljenovic T, Davenport M, Hulme J, et al. Heterogeneous silicon photonic integrated circuits. J Lightwave Technol 2016;34:20–35.
[15] Heck MJR, Bauters JF, Davenport ML, et al. Hybrid silicon photonic integrated circuit technology. IEEE J Sel Top Quantum 2013;19:6100117.
[16] Wörhoff K, Heideman RG, Leinse A, Hoekman M. TriPleX: a versatile dielectric photonic platform. Adv Opt Technol 2015;4:189–207.
[17] Moss DJ, Morandotti R, Gaeta AL, Lipson M. New CMOS-compatible platforms based on silicon nitride and Hydex for nonlinear optics. Nat Photon 2013;7:597–607.
[18] Bogaerts W, De Heyn P, Van Vaerenbergh T, et al. Silicon microring resonators. Laser Photon Rev 2012;6:47–73.
[19] Zhang W, Yao J. Silicon-based integrated microwave photonics. IEEE J Quantum Electron 2016;52:1–12.
[20] Meint S, Xaveer L, Huub A, et al. An introduction to InP-based generic integration technology. Semicond Sci Technol 2014;29:083001.
[21] Smit M, van der Tol J, Hill M. Moore's law in photonics. Laser Photon Rev 2012;6:1–13.
[22] Wang Z, Tian B, Pantouvaki M, et al. Room-temperature InP distributed feedback laser array directly grown on silicon. Nat Photon 2015;9:837–42.
[23] Guarino A, Poberaj G, Rezzonico D, Degl'Innocenti R, Gunter P. Electro-optically tunable microring resonators in lithium niobate. Nat Photon 2007;1:407–10.
[24] Chen C, Niu X, Han C, et al. Monolithic multi-functional integration of ROADM modules based on polymer photonic lightwave circuit. Opt Express 2014;22:10716–27.
[25] Teng J, Dumon P, Bogaerts W, et al. Athermal silicon-on-insulator ring resonators by overlaying a polymer cladding on narrowed waveguides. Opt Express 2009;17:14627–33.

[26] Eggleton BJ, Poulton CG, Pant R. Inducing and harnessing stimulated Brillouin scattering in photonic integrated circuits. Adv Opt Photonics 2013;5:536–87.
[27] Haffner C, Heni W, Fedoryshyn Y, et al. All-plasmonic Mach-Zehnder modulator enabling optical high-speed communication at the microscale. Nat Photon 2015;9:525–8.
[28] Fandiño JS, Muñoz P, Doménech D, Capmany J. A monolithic integrated photonic microwave filter. Nat Photon 2017;11:124–9.
[29] Metcalf AJ, Kim H-J, Leaird DE, et al. Integrated line-by-line optical pulse shaper for high-fidelity and rapidly reconfigurable RF-filtering. Opt Express 2016;24:23925–40.
[30] Feng S, Qin C, Shang K, et al. Rapidly reconfigurable high-fidelity optical arbitrary waveform generation in heterogeneous photonic integrated circuits. Opt Express 2017;25:-8872–85.
[31] Yamazaki H, Sano A, Nagatani M, Miyamoto Y. Single-carrier 1-Tb/s PDM-16QAM transmission using high-speed InP MUX-DACs and an integrated OTDM modulator. Opt Express 2015;23:12866–73.
[32] Fan Y, Epping JP, Oldenbeuving RM, et al. Optically integrated InP–Si_3N_4 hybrid laser. IEEE Photon J 2016;8:1–11.
[33] Chang L, Pfeiffer MHP, Volet N, et al. Heterogeneous integration of lithium niobate and silicon nitride waveguides for wafer-scale photonic integrated circuits on silicon. Opt Lett 2017;42:803–6.
[34] Sedra AS, Smith KC. Microelectronic circuits (The Oxford series in electrical and computer engineering). 7th ed. London, London, Oxford University Press, 2014.
[35] Nagarajan R, Joyner CH, Schneider RP, et al. Large-scale photonic integrated circuits. IEEE J Sel Top Quantum 2005;11:50–65.
[36] Harris NC, Bunandar D, Pant M, et al. Large-scale quantum photonic circuits in silicon. Nanophotonics 2016;5:456–68.
[37] Coldren LA, Corzine SW, Mashanovitch ML. Diode lasers and photonic integrated circuits. Hoboken, NJ, John Wiley & Sons, 2012.
[38] Zhuang L, Marpaung D, Burla M, Beeker W, Leinse A, Roeloffzen C. Low-loss, high-index-contrast Si3N4/SiO2 optical waveguides for optical delay lines in microwave photonics signal processing. Opt Express 2011;19:23162–70.
[39] Capmany J, Ortega B, Pastor D. A tutorial on microwave photonic filters. J Lightwave Technol 2006;24:201–29.
[40] Burla M, Li M, Cortés LR, et al. Terahertz-bandwidth photonic fractional Hilbert transformer based on a phase-shifted waveguide Bragg grating on silicon. Opt Lett 2014;39:6241–4.
[41] Wang WT, Liu JG, Sun WH, Wang WY, Wang SL, Zhu NH. Widely tunable single bandpass microwave photonic filter based on Brillouin-assisted optical carrier recovery. Opt Express 2014;22:29304–13.
[42] Supradeepa VR, Long CM, Wu R, et al. Comb-based radiofrequency photonic filters with rapid tunability and high selectivity. Nat Photon 2012;6:186–94.
[43] Capmany J, Doménech D, Muñoz P. Graphene integrated microwave photonics. J Lightwave Technol 2014;32:3785–96.
[44] Marpaung D, Morrison B, Pagani M, et al. Low-power, chip-based stimulated Brillouin scattering microwave photonic filter with ultrahigh selectivity. Optica 2015;2:76–83.
[45] Zhuang L, Roeloffzen CGH, Hoekman M, Boller K-J, Lowery AJ. Programmable photonic signal processor chip for radiofrequency applications. Optica 2015;2:854–9.
[46] Torres-Company V, Weiner AM. Optical frequency comb technology for ultra-broadband radio-frequency photonics. Laser Photon Rev 2014;8:368–93.
[47] Xue X, Zheng X, Zhang H, Zhou B. Widely tunable single-bandpass microwave photonic filter employing a non-sliced broadband optical source. Opt Express 2011;19:18423–9.
[48] Madsen CK, Zhao JH. Optical filter design and analysis: a signal processing approach. 1st ed. New York, Wiley, 1999.
[49] Bolea M, Mora J, Ortega B, Capmany J. Highly chirped single-bandpass microwave photonic filter with reconfiguration capabilities. Opt Express 2011;19:4566–76.
[50] Chan EHW, Minasian RA. Coherence-free high-resolution RF/microwave photonic bandpass filter with high skirt selectivity and high stopband attenuation. J Lightwave Technol 2010;28:1646–51.
[51] Chen H. Ultra-wideband microwave photonic filter with a high Q-factor using a semiconductor optical amplifier. Opt Lett 2017;42:1397–400.
[52] Rasras MS, Tu KY, Gill DM, et al. Demonstration of a tunable microwave-photonic notch filter using low-loss silicon ring resonators. J Lightwave Technol 2009;27:2105–10.
[53] Adar R, Serbin MR, Mizrahi V. Less than 1 dB per meter propagation loss of silica waveguides measured using a ring resonator. J Lightwave Technol 1994;12:1369–72.
[54] Melloni A, Costa R, Cusmai G, Morichetti F. The role of index contrast in dielectric optical waveguides. Int J Mater Prod Technol 2009;34:421–37.
[55] Zhuang L, Zhu C, Corcoran B, et al. Sub-GHz-resolution C-band Nyquist-filtering interleaver on a high-index-contrast photonic integrated circuit. Opt Express 2016;24:5715–27.
[56] Burla M, Marpaung D, Zhuang L, et al. On-chip CMOS compatible reconfigurable optical delay line with separate carrier tuning for microwave photonic signal processing. Opt Express 2011;19:21475–84.
[57] Ghelfi P, Laghezza F, Scotti F, et al. A fully photonics-based coherent radar system. Nature 2014;507:341–5.
[58] Yao J, Zeng F, Wang Q. Photonic generation of ultrawideband signals. J Lightwave Technol 2007;25:3219–35.
[59] Morichetti F, Ferrari C, Canciamilla A, Melloni A. The first decade of coupled resonator optical waveguides: bringing slow light to applications. Laser Photon Rev 2012;6:74–96.
[60] Palací J, Villanueva GE, Galan JV, Marti J, Vidal B. Single bandpass photonic microwave filter based on a notch ring resonator. IEEE Photon Technol Lett 2010;22:1276–8.
[61] Marpaung D, Morrison B, Pant R, et al. Si3N4 ring resonator-based microwave photonic notch filter with an ultrahigh peak rejection. Opt Express 2013;21:23286–94.
[62] Liu Y, Marpaung D, Choudhary A, Eggleton BJ. Lossless and high-resolution RF photonic notch filter. Opt Lett 2016;41:5306–9.
[63] Zhuang L. Flexible RF filter using a nonuniform SCISSOR. Opt Lett 2016;41:1118–21.
[64] Zhuang L, Taddei C, Hoekman M, et al. Ring resonator-based on-chip modulation transformer for high-performance phase-modulated microwave photonic links. Opt Express 2013;21:25999–6013.
[65] Zhuang L, Khan MR, Beeker W, Leinse A, Heideman R, Roeloffzen C. Novel microwave photonic fractional Hilbert trans-

former using a ring resonator-based optical all-pass filter. Opt Express 2012;20:26499–510.
[66] Zhuang L, Hoekman M, Beeker W, et al. Novel low-loss waveguide delay lines using Vernier ring resonators for on-chip multi-λ microwave photonic signal processors. Laser Photon Rev 2013;7:994–1002.
[67] Zhuang L, Roeloffzen CGH, Meijerink A, et al. Novel ring resonator-based integrated photonic beamformer for broadband phased array receive antennas—part II: experimental prototype. J Lightwave Technol 2010;28:19–31.
[68] Schippers H, Verpoorte J, Jorna P, et al. Broadband conformal phased array with optical beam forming for airborne satellite communication. Big Sky Resort, MT, USA, Paper presented at 2008 IEEE Aerospace Conference, 2008, pp. 1–8.
[69] Meijerink A, Roeloffzen CGH, Meijerink R, et al. Novel ring resonator-based integrated photonic beamformer for broadband phased array receive antennas—part I: design and performance analysis. J Lightwave Technol 2010;28:3–18.
[70] Zhuang L, Roeloffzen CGH, Heideman RG, Borreman A, Meijerink A, Etten WV. Single-chip ring resonator-based 1×8 optical beam forming network in CMOS-compatible waveguide technology. IEEE Photon Technol Lett 2007;19:1130–2.
[71] Zhuang L, Hoekman M, Taddei C, et al. On-chip microwave photonic beamformer circuits operating with phase modulation and direct detection. Opt Express 2014;22:17079–91.
[72] Burla M, Marpaung DAI, Zhuang L, et al. Multiwavelength-integrated optical beamformer based on wavelength division multiplexing for 2-D phased array antennas. J Lightwave Technol 2014;32:3509–20.
[73] Burla M, Roeloffzen CGH, Zhuang L, et al. System integration and radiation pattern measurements of a phased array antenna employing an integrated photonic beamformer for radio astronomy applications. Appl Opt 2012;51:789–802.
[74] Taddei C, Zhuang L, Hoekman M, et al. Fully reconfigurable coupled ring resonator-based bandpass filter for microwave signal processing. Sapporo, Japan, Paper presented at Microwave Photonics (MWP) and the 2014 9th Asia-Pacific Microwave Photonics Conference (APMP) International Topical Meeting, 2014, pp. 20–23.
[75] Yu H, Chen M, Guo Q, et al. Si3N4-based integrated optical analog signal processor and its application in RF photonic frontend. IEEE Photon J 2015;7:1–9.
[76] Taddei C, Yen NTH, Zhuang L, et al. Waveguide filter-based on-chip differentiator for microwave photonic signal processing. Alexandria, VA, USA: Paper presented at IEEE International Topical Meeting on Microwave Photonics (MWP), 2013, pp. 28–31.
[77] Zhuang L, Hoekman M, Oldenbeuving RM, Boller KJ, Roeloffzen CGH. CRIT-alternative narrow-passband waveguide filter for microwave photonic signal processors. IEEE Photon Technol Lett 2014;26:1034–7.
[78] Zhuang L, Burla M, Taddei C, et al. Integrated microwave photonic splitter with reconfigurable amplitude, phase, and delay offsets. Opt Lett 2015;40:5618–21.
[79] Zhuang L, Beeker W, Leinse A, Heideman R, van Dijk P, Roeloffzen C. Novel wideband microwave polarization network using a fully-reconfigurable photonic waveguide interleaver with a two-ring resonator-assisted asymmetric Mach-Zehnder structure. Opt Express 2013;21:3114–24.
[80] Lowery AJ, Zhuang L, Corcoran B, Zhu C, Xie Y. Photonic circuit topologies for optical OFDM and Nyquist WDM. J Lightwave Technol 2017;35:781–91.
[81] Tomkos I, Azodolmolky S, Solé-Pareta J, Careglio D, Palkopoulou E. A tutorial on the flexible optical networking paradigm: state of the art, trends, and research challenges. Proc IEEE 2014;102:1317–37.
[82] Zhuang L, Zhu C, Xie Y, et al. Nyquist-filtering (de)multiplexer using a ring resonator assisted interferometer circuit. J Lightwave Technol 2016;34:1732–8.
[83] Corcoran B, Zhu C, Schröder J, et al. Multipass performance of a chip-enhanced WSS for Nyquist-WDM sub-band switching. J Lightwave Technol 2016;34:1824–30.
[84] Geng Z, Xie Y, Zhuang L, et al. Photonic integrated circuit implementation of a sub-GHz-selectivity frequency comb filter for optical clock multiplication. Opt Express 2017;25:27635–45.
[85] Parker JS, Bhardwaj A, Binetti PRA, Hung YJ, Coldren LA. Monolithically integrated gain-flattened ring mode-locked laser for comb-line generation. IEEE Photon Technol Lett 2012;24:131–3.
[86] Carolan J, Harrold C, Sparrow C, et al. Universal linear optics. Science 2015;349:711–6.
[87] Editorial, Birth of the programmable optical chip. Nat Photon 2016;10:1.
[88] Pérez D, Gasulla I, Capmany J, Soref RA. Reconfigurable lattice mesh designs for programmable photonic processors. Opt Express 2016;24:12093–106.
[89] Wang J, Shen H, Fan L, et al. Reconfigurable radio-frequency arbitrary waveforms synthesized in a silicon photonic chip. Nat Commun 2015;6:5957.
[90] Chen S, Shi Y, He S, Dai D. Low-loss and broadband 2×2 silicon thermo-optic Mach-Zehnder switch with bent directional couplers. Opt Lett 2016;41:836–9.
[91] Suzuki K, Tanizawa K, Suda S, et al. Broadband silicon photonics 8×8 switch based on double-Mach-Zehnder element switches. Opt Express 2017;25:7538–46.
[92] Miller DAB. Perfect optics with imperfect components. Optica 2015;2:747–50.
[93] Capmany J, Gasulla I, Perez D. Microwave photonics: the programmable processor. Nat Photon 2016;10:6–8.
[94] Pérez D, Gasulla I, Capmany J. Software-defined reconfigurable microwave photonics processor. Opt Express 2015;23:14640–54.
[95] Langrock C, Kumar S, McGeehan JE, Willner AE, Fejer MM. All-optical signal processing using χ^2 nonlinearities in guided-wave devices. J Lightwave Technol 2006;24:2579–92.
[96] Liu W, Li M, Guzzon RS, et al. A fully reconfigurable photonic integrated signal processor. Nat Photon 2016;10:190–5.
[97] Roeloffzen C, Oldenbeuving R, Timens RB, et al. Integrated optical beamformers. Los Angeles, CA, USA, Paper presented at Optical Fiber Communication Conference, 2015, p. ThA2.
[98] Rasras MS, Gill DM, Patel SS, et al. Demonstration of a fourth-order pole-zero optical filter integrated using CMOS processes. J Lightwave Technol 2007;25:87–92.
[99] Dong P, Feng N-N, Feng D, et al. GHz-bandwidth optical filters based on high-order silicon ring resonators. Opt Express 2010;18:23784–9.

[100] Orlandi P, Morichetti F, Strain MJ, Sorel M, Bassi P, Melloni A. Photonic integrated filter with widely tunable bandwidth. J Lightwave Technol 2014;32:897–907.
[101] Ibrahim S, Fontaine NK, Djordjevic SS, et al. Demonstration of a fast-reconfigurable silicon CMOS optical lattice filter. Opt Express 2011;19:13245–56.
[102] Guan B, Djordjevic SS, Fontaine NK, et al. CMOS compatible reconfigurable silicon photonic lattice filters using cascaded unit cells for RF-photonic processing. IEEE J Sel Top Quantum 2014;20:359–68.
[103] Norberg EJ, Guzzon RS, Nicholes SC, Parker JS, Coldren LA. Programmable photonic lattice filters in InGaAsP-InP. IEEE Photon Technol Lett 2010;22:109–111.
[104] Guzzon RS, Norberg EJ, Parker JS, Johansson LA, Coldren LA. Integrated InP-InGaAsP tunable coupled ring optical bandpass filters with zero insertion loss. Opt Express 2011;19:7816–26.
[105] Chen HW, Fang AW, Peters JD, et al. Integrated microwave photonic filter on a hybrid silicon platform. IEEE Trans Microw Theory Tech 2010;58:3213–9.
[106] Sancho J, Bourderionnet J, Lloret J, et al. Integrable microwave filter based on a photonic crystal delay line. Nat Commun 2012;3:1075.
[107] Wabnitz S, Eggleton BJ. All-optical signal processing: data communication and storage applications, 1st ed. Basel, Springer, 2015.
[108] Ziyadi M, Mohajerin-Ariaei A, Chitgarha MR, et al. Tunable radio frequency photonics filter using a comb-based optical tapped delay line with an optical nonlinear multiplexer. Opt Lett 2015;40:3284–7.
[109] Morrison B, Marpaung D, Pant R, et al. Tunable microwave photonic notch filter using on-chip stimulated Brillouin scattering. Opt Commun 2014;313:85–9.
[110] Byrnes A, Pant R, Li E, et al. Photonic chip based tunable and reconfigurable narrowband microwave photonic filter using stimulated Brillouin scattering. Opt Express 2012;20:18836–45.
[111] Choudhary A, Aryanfar I, Shahnia S, et al. Tailoring of the Brillouin gain for on-chip widely tunable and reconfigurable broadband microwave photonic filters. Opt Lett 2016;41:436–9.
[112] Casas-Bedoya A, Morrison B, Pagani M, Marpaung D, Eggleton BJ. Tunable narrowband microwave photonic filter created by stimulated Brillouin scattering from a silicon nanowire. Opt Lett 2015;40:4154–7.
[113] Tu KY, Rasras MS, Gill DM, et al. Silicon RF-photonic filter and down-converter. J Lightwave Technol 2010;28:3019–28.
[114] Alipour P, Eftekhar AA, Atabaki AH, et al. Fully reconfigurable compact RF photonic filters using high-Q silicon microdisk resonators. Opt Express 2011;19:15899–907.
[115] Dong J, Liu L, Gao D, et al. Compact notch microwave photonic filters using on-chip integrated microring resonators. IEEE Photon J 2013;5:5500307.
[116] Long Y, Zhang H, Li C, Gui C, Yang Q, Wang J. Ultra-high peak rejection notch microwave photonic filter using a single silicon microring resonator. Los Angeles, CA, USA, Paper presented at Optical Fiber Communication Conference, 2015, p. W2A.58.
[117] Doylend JK, Heck MJR, Bovington JT, et al. Hybrid III/V silicon photonic source with integrated 1D free-space beam steering. Opt Lett 2012;37:4257–9.
[118] Morichetti F, Grillanda S, Melloni A. Breakthroughs in photonics 2013: toward feedback-controlled integrated photonics. IEEE Photon J 2014;6:1–6.
[119] Li Y, Zhang Y, Huang Y. Any bias point control technique for Mach-Zehnder modulator. IEEE Photon Technol Lett 2013;25:2412–5.
[120] Grillanda S, Carminati M, Morichetti F, et al. Non-invasive monitoring and control in silicon photonics using CMOS integrated electronics. Optica 2014;1:129–36.
[121] Annoni A, Guglielmi E, Carminati M, et al. Automated routing and control of silicon photonic switch fabrics. IEEE J Sel Top Quantum 2016;22:169–76.
[122] Miller DAB. Designing linear optical components. Opt Photonics News 2013;24:38.
[123] Miller DAB. Reconfigurable add-drop multiplexer for spatial modes. Opt Express 2013;21:20220–9.
[124] Cheng Q, Stabile R, Rohit A, et al. First demonstration of automated control and assessment of a dynamically reconfigured monolithic 8×8 wavelength-and-space switch. IEEE J Opt Commun Netw 2015;7:A388–95.
[125] Alipour P, Hosseini ES, Eftekhar AA, Momeni B, Adibi A. Athermal performance in high-Q polymer-clad silicon microdisk resonators. Opt Lett 2010;35:3462–64.
[126] Zhou L, Okamoto K, Yoo SJB. Athermalizing and trimming of slotted silicon microring resonators with UV-sensitive PMMA upper-cladding. IEEE Photon Technol Lett 2009;21:1175–7.
[127] Djordjevic SS, Shang K, Guan B, et al. CMOS-compatible, athermal silicon ring modulators clad with titanium dioxide. Opt Express 2013;21:13958–68.
[128] Hosseini N, Dekker R, Hoekman M, et al. Stress-optic modulator in TriPleX platform using a piezoelectric lead zirconate titanate (PZT) thin film. Opt Express 2015;23:14018–26.
[129] Pérez D, Gasulla I, Crudgington L, et al. Multipurpose silicon photonics signal processor core. Nat Commun 2017;8:636.
[130] Pérez D, Gasulla I, Javier Fraile F, et al. Silicon photonics rectangular universal interferometer. Laser Photo Rev 2017;11:1700219.